

Stability of triple diffusive convection in a viscoelastic fluid-saturated porous layer*K. R. RAGHUNATHA, I. S. SHIVAKUMARA[†]

Department of Mathematics, Bangalore University, Bangalore 560056, India

(Received Jan. 14, 2018 / Revised Apr. 24, 2018)

Abstract The triple diffusive convection in an Oldroyd-B fluid-saturated porous layer is investigated by performing linear and weakly nonlinear stability analyses. The condition for the onset of stationary and oscillatory is derived analytically. Contrary to the observed phenomenon in Newtonian fluids, the presence of viscoelasticity of the fluid is to degenerate the quasiperiodic bifurcation from the steady quiescent state. Under certain conditions, it is found that disconnected closed convex oscillatory neutral curves occur, indicating the requirement of three critical values of the thermal Darcy-Rayleigh number to identify the linear instability criteria instead of the usual single value, which is a novel result enunciated from the present study for an Oldroyd-B fluid saturating a porous medium. The similarities and differences of linear instability characteristics of Oldroyd-B, Maxwell, and Newtonian fluids are also highlighted. The stability of oscillatory finite amplitude convection is discussed by deriving a cubic Landau equation, and the convective heat and mass transfer are analyzed for different values of physical parameters.

Key words Oldroyd-B fluid, bifurcation, instability, perturbation method, nonlinear stability, heat and mass transfer

Chinese Library Classification O357.3, O175.8

2010 Mathematics Subject Classification 76E06, 76A10, 76S05

Nomenclature

d ,	depth of the porous layer;	Pr_D ,	Darcy-Prandtl number;
g ,	gravitational acceleration;	\mathbf{q} ,	velocity vector;
K ,	permeability of the porous medium;	Rs_i ,	solute Darcy-Rayleigh number of the i th-component;
\mathbf{k} ,	unit vector in the vertical direction;	R_T ,	thermal Darcy-Rayleigh number;
M ,	ratio of heat capacities;	t ,	time;
p ,	pressure;	x, y, z ,	space coordinates.

* Citation: RAGHUNATHA, K. R. and SHIVAKUMARA, I. S. Stability of triple diffusive convection in a viscoelastic fluid-saturated porous layer. *Applied Mathematics and Mechanics (English Edition)*, **39**(10), 1385–1410 (2018) <https://doi.org/10.1007/s10483-018-2376-8>

[†] Corresponding author, E-mail: shivakumarais@bub.ernet.in

Project supported by the Innovation in Science Pursuit for the Inspired Research (INSPIRE) Program (No. DST/INSPIRE Fellowship/[IF 150253])

Greek symbols

α ,	horizontal wave number;	Λ_1 ,	stress relaxation parameter;
α_T ,	thermal expansion coefficient;	Λ_2 ,	strain retardation parameter;
α_{Si} ,	solute analogue of α_T , $i = 1, 2$;	μ ,	dynamic viscosity;
ε ,	porosity;	ν ,	kinematic viscosity;
κ_T ,	thermal diffusivity;	ρ ,	fluid density;
κ_{Si} ,	solute diffusivity, $i = 1, 2$;	σ ,	growth term;
λ_1 ,	stress relaxation time;	τ_i ,	ratio of diffusivities, $i = 1, 2$;
λ_2 ,	strain retardation time;	ψ ,	stream function.

Subscripts/superscripts

b,	basic state;	U,	upper boundary;
L,	lower boundary;	*	dimensionless variable.

1 Introduction

The study of convective instabilities is one of the central problems in porous media fluid mechanics because of its natural occurrence and relevance in many science and engineering applications. It is a well-established fact that, in a horizontal porous layer, thermal instability sets in as stationary convection, and no oscillatory motion takes place^[1-2]. Nonetheless, in the case of double diffusive convection, it is intriguing to note that oscillatory convection appears as a preferred mode of instability under some conditions. Copious literatures available on these topics are documented in the books^[3-6].

Of late, researchers have been showing an increasing attention in the study of natural convection of non-Newtonian fluids saturating porous media, and the studies are very sparse. Most of the existing studies have focused on thermal convective instability in a viscoelastic fluid-saturated porous layer^[7-10] as applications of these fluids are found in geophysics, biorheology, pharmaceutical and petroleum industries, polymer processing and so on. An important result noticed that the fluid elasticity influences the preferred mode of instability from the stationary mode to the oscillatory mode. Besides, investigations have also been carried out to investigate the consequence of additional diffusing component (double diffusive convection) on thermal convective instability in a viscoelastic fluid-saturated porous layer^[11-13].

Convective instability in ternary fluids is a complex process, and the presence of thermal currents and/or concentrations leads to linear and nonlinear behaviours. In a ternary fluid, the density depends on three different stratifying agents, and one of which may be the temperature. This leads to a competition between different diffusions of stratifying agents, and as a result, oscillatory convection may occur. Triple diffusive convection is found to occur in many practical applications. For example, aqueous suspensions of deoxyribonucleic acid (DNA) may contain more than two independently diffusing components with different diffusivities. The DNA coils are bound to be extended as they are subject to the action of shear or externally applied tension, and as a result, the viscoelastic properties of DNA are to be taken into consideration in the study of DNA convection. Although the oscillatory convection in viscoelastic fluids is not observed in experimental conditions^[14], Perkins et al.^[15-16] showed that such a convection persists as the first convective instability in dilute suspensions of long DNA molecules. Later, Kolodner^[17] also confirmed this possibility. Another important situation stems from the study of medical screening tool for abnormalities in lipids, containing various components such as cholesterol (low-density lipoproteins, high-density lipoproteins) and triglycerides which possess different diffusivities and exhibit viscoelastic properties. These proteins and fats help to generate energy in the human body, and this complex process is collectively known as cellular respiration. In particular, the variations in these diffusivities help to determine approximate

risks for cardiovascular and other diseases. Another area of interest is in understanding contaminant transport^[18–19], where the chemical species that form the contaminants are non-reactive. These observations have triggered a renewed interest in the study of linear and nonlinear convective instabilities in viscoelastic triple diffusive fluid systems.

The triple diffusive convection in a Newtonian fluid layer has been studied extensively^[20–27]. In particular, Pearlstein et al.^[24] discussed several applications and established some novel results which were overlooked by the previous investigators and also not found in double diffusive fluid systems. Shivakumara and Naveen-Kumar^[28] investigated linear and nonlinear multi-diffusive convection in a horizontal layer of couple stress fluids. The study of triple diffusive convection in porous media has also been analyzed. Rudraiah and Vortmeyer^[29] and Poulikakos^[30] studied the onset of triple diffusive convection in a porous medium by following the analysis of Griffiths^[20]. Whereas Tracey^[31] followed the analysis of Pearlstein et al.^[24] to study the triple diffusive convection in porous media, and Rionero^[32–33] extended the study to obtain some additional results. The linear instability of the triple diffusive Maxwell fluid-saturated porous layer was considered by Zhao et al.^[34] while a weakly nonlinear stability analysis of the problem has been investigated recently by Raghunatha et al.^[35].

The studies of convective instability in viscoelastic fluids saturating a porous medium are mainly focused either on single or double diffusive fluid systems despite the multi-diffusive convection is bound to occur in many practical situations mentioned above. As far as the Newtonian fluid systems are concerned, some fundamental differences between double and triple diffusive fluid systems in the onset and development of convective motion are unveiled. In light of these observations, it is pragmatic that to explore the qualitatively new features found by Tracey^[31] will carry over to the case of Oldroyd-B fluids saturating a porous medium as well since such a study sheds more light on the complex instability characteristics of the system. The objective of the current study is to investigate linear and weakly nonlinear triple diffusive convection in an Oldroyd-B fluid-saturated porous medium and to unveil some interesting results that the system is capable of supporting. Also, the main purpose is to understand the stability of oscillatory bifurcating solution by deriving a cubic Landau equation and also to understand the influence of various physical parameters on convective heat and mass transfer.

2 Governing equations

The physical configuration is shown in Fig. 1. We consider an incompressible Oldroyd-B type of a viscoelastic fluid-saturated horizontal layer of a Darcy porous medium of the thickness d containing three stratifying agents with different molecular diffusivities, where all the three may be solute concentrations, or one of the components may be the temperature T , and the other two are solute concentrations S_i ($i = 1, 2$). The lower impermeable boundary is kept at the higher temperature and solute concentrations, while at the upper impermeable boundary, they are maintained at lower values. A Cartesian coordinate system (x, y, z) is chosen such that the origin is at the bottom of the porous layer. The gravity is acting in the negative vertical z -direction. A condition of local thermal equilibrium between the solid phase and the fluid phase of the porous medium is assumed.

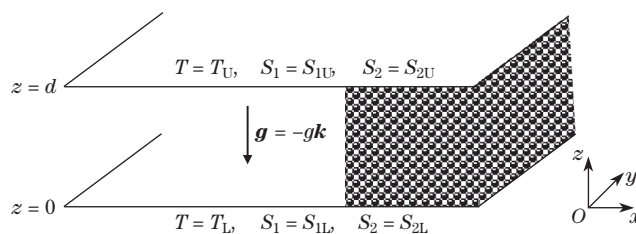


Fig. 1 Physical configuration

A modified Darcy-Oldroyd model relevant to the case of a Darcy porous medium has been considered to describe the flow in a porous medium in the form^[34–38] of

$$\left(1 + \lambda_1 \frac{\partial}{\partial t}\right) \left(\frac{\rho_0}{\varepsilon} \frac{\partial \mathbf{q}}{\partial t} + \nabla p - \rho \mathbf{g}\right) = -\frac{\mu}{K} \left(1 + \lambda_2 \frac{\partial}{\partial t}\right) \mathbf{q}, \tag{1}$$

where $\mathbf{q} = (u, v, w)$ is the velocity, p is the pressure, μ is the fluid viscosity, \mathbf{g} is the acceleration due to gravity, K is the permeability of the medium, ρ is the fluid density, ε is the porosity, λ_1 is the relaxation time, and λ_2 is the retardation time. It may be noted that the time derivative term has been included in the above equation as it contributes for the convection to set in as oscillatory motions. The viscoelastic model considered includes the classical viscous Newtonian fluid as a special case for $\lambda_1 = \lambda_2 = 0$ and the Maxwell fluid for $\lambda_2 = 0$. The conservation equations for the stratifying agents are

$$M \frac{\partial T}{\partial t} + (\mathbf{q} \cdot \nabla) T = \kappa_T \nabla^2 T, \tag{2}$$

$$\varepsilon \frac{\partial S_1}{\partial t} + (\mathbf{q} \cdot \nabla) S_1 = \kappa_{S1} \nabla^2 S_1, \tag{3}$$

$$\varepsilon \frac{\partial S_2}{\partial t} + (\mathbf{q} \cdot \nabla) S_2 = \kappa_{S2} \nabla^2 S_2, \tag{4}$$

where $M = (\rho_0 c)_m / (\rho_0 c)_f = ((1 - \varepsilon)(\rho_0 c)_s + \varepsilon(\rho_0 c)_f) / (\rho_0 c)_f$ is the ratio of heat capacities, c is the specific heat, κ_T is the thermal diffusivity, and κ_{S1} and κ_{S2} are the solute analogues of κ_T . The subscripts m, f, and s refer to the porous medium, fluid, and solid, respectively. Under the Oberbeck-Boussinesq approximation, the equation of state is

$$\rho = \rho_0 (1 - \alpha_T (T - T_L) + \alpha_{S1} (S_1 - S_{1L}) + \alpha_{S2} (S_2 - S_{2L})), \tag{5}$$

where α_T is the thermal expansion coefficient, α_{S1} and α_{S2} are the solute analogues of α_T , and ρ_0 is the density at the reference temperature and solute concentrations.

The boundary conditions are

$$\mathbf{q} \cdot \mathbf{k} = 0 \quad \text{at} \quad z = 0, d, \tag{6}$$

$$(T, S_i) = (T_L, S_{iL}) \quad \text{at} \quad z = 0, \tag{7}$$

$$(T, S_i) = (T_U, S_{iU}) \quad \text{at} \quad z = d \quad (i = 1, 2), \tag{8}$$

where $S_{iU} < S_{iL}$ and $T_U < T_L$ with the sign convention that $\Delta S_i = S_{iL} - S_{iU} > 0$ when a solute concentration is stabilizing and $\Delta T = T_L - T_U > 0$ when the temperature is destabilizing.

The above governing equations are made dimensionless using the following transformations:

$$\begin{cases} \nabla^* = d \nabla, & \mathbf{q}^* = \frac{d}{\kappa_T} \mathbf{q}, & p^* = \frac{K}{\mu \kappa_T} p, & t^* = \frac{\kappa_T}{d^2 \varepsilon} t, \\ T^* = \frac{T - T_L}{\Delta T}, & S_i^* = \frac{S - S_{iL}}{\Delta S_i} \quad (i = 1, 2). \end{cases} \tag{9}$$

Substituting Eq. (9) into the governing equations, we obtain

$$\left(1 + \Lambda_1 \frac{\partial}{\partial t}\right) \left(\frac{1}{Pr_D} \frac{\partial \mathbf{q}}{\partial t} + \nabla p + (-R_T T + R_{S1} S_1 + R_{S2} S_2) \mathbf{k}\right) = -\left(1 + \Lambda_2 \frac{\partial}{\partial t}\right) \mathbf{q}, \tag{10}$$

$$A \frac{\partial T}{\partial t} + (\mathbf{q} \cdot \nabla) T = \nabla^2 T, \tag{11}$$

$$\frac{\partial S_1}{\partial t} + (\mathbf{q} \cdot \nabla) S_1 = \tau_1 \nabla^2 S_1, \tag{12}$$

$$\frac{\partial S_2}{\partial t} + (\mathbf{q} \cdot \nabla) S_1 = \tau_2 \nabla^2 S_1, \tag{13}$$

where $\Lambda_1 = \lambda_1 \kappa_T / (d^2 \varepsilon)$ is the stress relaxation time parameter, $\Lambda_2 = \lambda_2 \kappa_T / (d^2 \varepsilon)$ is the strain retardation time parameter, $R_T = \alpha_T g \Delta T K d / (\nu \kappa_T)$ is the thermal Darcy-Rayleigh number, $R_{S_i} = \alpha_{S_i} g \Delta S_i K d / (\nu \kappa_T)$ ($i = 1, 2$) is the solute Darcy-Rayleigh number of the i th-component, $Pr_D = \nu d^2 \varepsilon^2 / (\kappa_T K)$ is the Darcy-Prandtl number or the Vadasz number, $\tau_i = \kappa_{S_i} / \kappa_T$ ($i = 1, 2$) is the ratio of diffusivities, and $A = M / \varepsilon$. If all the components are solute concentrations, then the value of A turns out to be unity. The basic state is quiescent, and temperature, solute concentrations, and pressure distributions are found to be

$$T_b(z) = -z, \quad S_{ib}(z) = -z \quad (i = 1, 2), \quad p_b(z) = p_0 + (R_{S1} + R_{S2} - R_T)z^2/2, \quad (14)$$

where p_0 is the pressure at $z = 0$, and the subscript b denotes the basic state. To investigate the instability of the basic state, we now superimpose infinitesimal perturbations on the basic state of the form,

$$\mathbf{q} = 0 + \mathbf{q}', \quad p = p_b(z) + p', \quad T = T_b(z) + T', \quad S_i = S_{ib}(z) + S'_{ib} \quad (i = 1, 2), \quad (15)$$

where primes indicate the perturbed quantities. Substituting Eq. (15) into Eqs. (10)–(13), eliminating the pressure term from the momentum equation by operating curl and introducing a perturbation stream function $\psi'(x, y, z)$ with

$$u' = \frac{\partial \psi'}{\partial z}, \quad w' = -\frac{\partial \psi'}{\partial x}, \quad (16)$$

we obtain the governing nonlinear stability equations which can be written as

$$L \begin{bmatrix} \psi \\ T \\ S_1 \\ S_2 \end{bmatrix} = \begin{bmatrix} 0 \\ J(\psi, T) \\ J(\psi, S_1) \\ J(\psi, S_2) \end{bmatrix}, \quad (17)$$

where $J(\cdot, \cdot)$ is the Jacobian function with respect to x and z , representing the nonlinear terms, and L is the linear differential operator given by

$$L = \begin{bmatrix} \frac{1}{Pr_D} \frac{\partial}{\partial t} \nabla^2 + \frac{\left(1 + \Lambda_2 \frac{\partial}{\partial t}\right)}{\left(1 + \Lambda_1 \frac{\partial}{\partial t}\right)} \nabla^2 & R_T \frac{\partial}{\partial x} & -R_{S1} \frac{\partial}{\partial x} & -R_{S2} \frac{\partial}{\partial x} \\ \frac{\partial}{\partial x} & A \frac{\partial}{\partial t} - \nabla^2 & 0 & 0 \\ \frac{\partial}{\partial x} & 0 & \frac{\partial}{\partial t} - \tau_1 \nabla^2 & 0 \\ \frac{\partial}{\partial x} & 0 & 0 & \frac{\partial}{\partial t} - \tau_2 \nabla^2 \end{bmatrix}, \quad (18)$$

where $\nabla^2 = \frac{\partial^2}{\partial x^2} + \frac{\partial^2}{\partial z^2}$.

The boundary conditions now become

$$\psi = T = S_1 = S_2 = 0 \quad \text{at} \quad z = 0, 1. \quad (19)$$

3 Linear instability analysis

The linear instability analysis proceeds by ignoring the nonlinear terms in Eq. (17). Then, we eliminate T , S_1 , and S_2 from the momentum equation to provide one equation for ψ in the form,

$$\begin{aligned} & \left(\frac{\partial}{\partial t} - \tau_1 \nabla^2 \right) \left(\frac{\partial}{\partial t} - \tau_2 \nabla^2 \right) \left(\left(A \frac{\partial}{\partial t} - \nabla^2 \right) \left(\frac{1}{Pr_D} \frac{\partial}{\partial t} \left(1 + \Lambda_1 \frac{\partial}{\partial t} \right) \nabla^2 + \left(1 + \Lambda_2 \frac{\partial}{\partial t} \right) \right) \nabla^2 \psi \right) \\ & - R_T \left(1 + \Lambda_1 \frac{\partial}{\partial t} \right) \left(\frac{\partial}{\partial t} - \tau_1 \nabla^2 \right) \left(\frac{\partial}{\partial t} - \tau_2 \nabla^2 \right) \frac{\partial^2 \psi}{\partial x^2} + \left(1 + \Lambda_1 \frac{\partial}{\partial t} \right) \left(A \frac{\partial}{\partial t} - \nabla^2 \right) \\ & \cdot \left(R_{S1} \left(\frac{\partial}{\partial t} - \tau_2 \nabla^2 \right) + R_{S2} \left(\frac{\partial}{\partial t} - \tau_1 \nabla^2 \right) \right) \frac{\partial^2 \psi}{\partial x^2} = 0. \end{aligned} \quad (20)$$

As usual, a normal mode solution is assumed as

$$\psi = e^{\sigma t} \sin(\alpha x) \sin(\pi z), \quad (21)$$

where α and π are wave numbers in the x - and z -directions, respectively, and $\sigma (= \sigma_r + i\omega)$ is the growth term. Substituting Eq. (21) into Eq. (20) yields the following expression:

$$R_T = \frac{A\sigma + \delta^2}{\sigma + \tau_1 \delta^2} R_{S1} + \frac{A\sigma + \delta^2}{\sigma + \tau_2 \delta^2} R_{S2} + \frac{A\sigma + \delta^2}{\alpha^2} \left(\frac{1 + \Lambda_2 \sigma}{1 + \Lambda_1 \sigma} \delta^2 + \frac{\sigma \delta^2}{Pr_D} \right), \quad (22)$$

where $\delta^2 = \alpha^2 + \pi^2$. To investigate the instability of the system, the real part of σ is set to zero, and let $\sigma = i\omega$ in Eq. (22) and also clear the complex quantities from the denominator to obtain

$$\begin{aligned} R_T = & \frac{\tau_1 \delta^4 + A\omega^2}{\omega^2 + \tau_1^2 \delta^4} R_{S1} + \frac{\tau_2 \delta^4 + A\omega^2}{\omega^2 + \tau_2^2 \delta^4} R_{S2} + \frac{\delta^4}{\alpha^2} \left(\frac{1 + \omega^2 \Lambda_1 \Lambda_2}{1 + \omega^2 \Lambda_1^2} \right) - \frac{A\omega^2 \delta^2}{\alpha^2} \left(\frac{\Lambda_2 - \Lambda_1}{1 + \omega^2 \Lambda_1^2} + \frac{1}{Pr_D} \right) \\ & + i\omega \delta^2 N, \end{aligned} \quad (23)$$

where

$$N = \frac{A\tau_1 - 1}{\omega^2 + \tau_1^2 \delta^4} R_{S1} + \frac{A\tau_2 - 1}{\omega^2 + \tau_2^2 \delta^4} R_{S2} + \frac{\delta^2}{\alpha^2} \left(\frac{\Lambda_2 - \Lambda_1}{1 + \omega^2 \Lambda_1^2} + \frac{1}{Pr_D} \right) + \frac{A}{\alpha^2} \left(\frac{1 + \omega^2 \Lambda_1 \Lambda_2}{1 + \omega^2 \Lambda_1^2} \right). \quad (24)$$

Since R_T is a physical quantity, it implies either $\omega = 0$ or $N = 0$ in Eq. (23). The condition $\omega = 0$ corresponds to the stationary convection, and the case $N = 0$ ($\omega \neq 0$) corresponds to the oscillatory convection.

3.1 Stationary convection

The condition $\omega = 0$ corresponds to the stationary onset, and thus

$$R_T^S = \frac{R_{S1}}{\tau_1} + \frac{R_{S2}}{\tau_2} + \frac{(\alpha^2 + \pi^2)^2}{\alpha^2} \quad (25)$$

is the thermal Darcy-Rayleigh number, where the layer is unstable with respect to the stationary onset. It is observed that Eq. (25) is independent of viscoelastic parameters, indicating that the viscoelastic effects appear only in the case of time dependent motions, and coincide with the result obtained for ordinary viscous fluids^[29]. We note that, for the stationary neutral solution, R_T^S is a single valued function of α and attains its critical value at $\alpha_c = \pi$. Therefore, the critical thermal Darcy-Rayleigh number for the stationary onset is

$$R_{Tc}^S = \frac{R_{S1}}{\tau_1} + \frac{R_{S2}}{\tau_2} + 4\pi^2. \quad (26)$$

In the absence of additional diffusing components, Eq. (26) gives $R_{Tc}^S = 4\pi^2$, which is the known exact value.

3.2 Oscillatory convection

For the oscillatory case, $\omega \neq 0$ and hence $N = 0$, which gives a dispersion relation cubic in ω^2 ,

$$a_1(\omega^2)^3 + a_2(\omega^2)^2 + a_3\omega^2 + a_4 = 0, \tag{27}$$

where

$$\begin{aligned} a_1 &= \delta^2\Lambda_1^2 + \Lambda_1\Lambda_2APr_D, \\ a_2 &= \alpha^2Pr_D(A\tau_1 - 1)\Lambda_1^2R_{S1} + \alpha^2Pr_D(A\tau_2 - 1)\Lambda_1^2R_{S2} + Pr_D\delta^2(\Lambda_2 - \Lambda_1) + \delta^2 \\ &\quad + (\tau_1^2 + \tau_2^2)\Lambda_1^2\delta^6 + APr_D + APr_D\Lambda_1\Lambda_2\delta^4(\tau_1^2 + \tau_2^2), \\ a_3 &= \alpha^2Pr_D(A\tau_1 - 1)(1 + \Lambda_1^2\tau_2^2\delta^4)R_{S1} + \alpha^2Pr_D(A\tau_2 - 1)(1 + \Lambda_1^2\tau_1^2\delta^4)R_{S2} + (\tau_1^2 + \tau_2^2)\delta^6 \\ &\quad + Pr_D\delta^6(\Lambda_2 - \Lambda_1)(\tau_1^2 + \tau_2^2) + \Lambda_1^2\tau_1^2\tau_2^2\delta^{10} + APr_D(\tau_1^2 + \tau_2^2)\delta^4 + APr_D\Lambda_1\Lambda_2\tau_1^2\tau_2^2\delta^8, \\ a_4 &= \alpha^2Pr_D(A\tau_1 - 1)\tau_2^2\delta^4R_{S1} + \alpha^2Pr_D(A\tau_2 - 1)\tau_1^2\delta^4R_{S2} + Pr_D\delta^{10}(\Lambda_2 - \Lambda_1)\tau_1^2\tau_2^2 \\ &\quad + \tau_1^2\tau_2^2\delta^{10} + APr_D\tau_1^2\tau_2^2\delta^8. \end{aligned}$$

When $N = 0$, Eq. (23) shows that the oscillatory convection occurs at $R_T = R_T^0$, where

$$R_T^0 = R_T^S - \omega^2 \left(\frac{(1 - A\tau_1)}{(\omega^2 + \tau_1^2\delta^4)} \frac{R_{S1}}{\tau_1} + \frac{(1 - A\tau_2)}{(\omega^2 + \tau_2^2\delta^4)} \frac{R_{S2}}{\tau_2} + \frac{A\delta^2}{\alpha^2Pr_D} - \frac{\delta^2}{\alpha^2} \frac{(A - \delta^2\Lambda_1)(\Lambda_1 - \Lambda_2)}{(1 + \omega^2\Lambda_1^2)} \right), \tag{28}$$

and ω^2 is given by Eq. (27). Equation (27) shows that, for a suitable combination of parameters $A, Pr_D, \Lambda_1, \Lambda_2, \tau_1, \tau_2, R_{S1}$, and R_{S2} , it is possible to have more than one positive values of ω^2 at the same wave number α , indicating the existence of the multiple oscillatory neutral solution R_T^0 which has important implications on the nature of the instability of the system. For a single diffusive case ($R_{S1} = R_{S2} = 0$), it is observed that the oscillatory convection occurs provided that

$$\omega^2 = \frac{\delta^2Pr_D(\Lambda_1 - \Lambda_2) - \delta^2 - APr_D}{\delta^2\Lambda_1^2 + APr_D\Lambda_1\Lambda_2} > 0. \tag{29}$$

Thus, the necessary condition for the occurrence of oscillatory convection is

$$\Lambda_1 - \Lambda_2 > \frac{1}{Pr_D} + \frac{A}{\delta^2}. \tag{30}$$

For a double diffusive case ($R_{S2} = 0$, say), we derive a dispersion relation quadratic in ω^2 ,

$$b_1(\omega^2)^2 + b_2\omega^2 + b_3 = 0, \tag{31}$$

where

$$\begin{aligned} b_1 &= \delta^2\Lambda_1^2 + \Lambda_1\Lambda_2APr_D, \\ b_2 &= \alpha^2Pr_D(A\tau_1 - 1)\Lambda_1^2R_{S1} + Pr_D\delta^2(\Lambda_2 - \Lambda_1) + (1 + \tau_1^2\Lambda_1^2\delta^4)\delta^2 + (1 + \tau_1^2\Lambda_1\Lambda_2\delta^4)APr_D, \\ b_3 &= \alpha^2Pr_D(A\tau_1 - 1)R_{S1} + (\Lambda_2 - \Lambda_1)\tau_1^2\delta^6Pr_D + \tau_1^2\delta^6 + \tau_1^2\delta^4APr_D. \end{aligned}$$

Since $\omega^2 > 0$ for the occurrence of oscillatory convection, a cautious glance at Eq. (31) provides the imminent conditions as

$$\tau_1 < \frac{1}{A}, \quad \Lambda_1 - \Lambda_2 > \frac{1}{Pr_D} + \frac{A}{\delta^2}. \tag{32}$$

The point at which the steady and oscillatory neutral curves meet is called the bifurcation point which can be located in the (α, R_T) plane. The bifurcation points will occur on the steady neutral curve at $\alpha = \alpha_b$ for which $\omega = 0$ satisfying Eq.(27). Thus, $a_4(\alpha_b) = 0$, or equivalently

$$\begin{aligned} &\varpi(\alpha_b^2)^3 + (3\pi^2\varpi + AP r_D)(\alpha_b^2)^2 + \left(3\pi^4\varpi + 2\pi^2 AP r_D + \varphi_1 \frac{R_{S1}}{\tau_1^2} + \varphi_2 \frac{R_{S2}}{\tau_2^2}\right)\alpha_b^2 \\ &+ \varpi\pi^6 + AP r_D\pi^2 = 0, \end{aligned} \tag{33}$$

where $\varphi_i = Pr_D(A\tau_i - 1)$ ($i = 1, 2$) and $\varpi = (\Lambda_2 - \Lambda_1)Pr_D + 1$. The minimum value of R_T^0 with respect to α , denoted by R_{Tc}^0 , is calculated using the procedure explained by Raghunatha et al.^[35].

4 Oscillatory nonlinear stability analysis

The linear instability theory discussed in the previous section gives us the condition for instability. Here, we use the perturbation method to perform the nonlinear stability analysis and derive the cubic Landau equation. Such a study helps to analyze the convective rate of heat and mass transfer. Since the viscoelastic effects are time dependent, the study has been restricted to the periodic convective solution that bifurcates at $R_T = R_{Tc}^0$. Accordingly, a small parameter χ that indicates the deviation from the critical point is introduced. Consequently, the stream function, temperature, and solute concentrations are expanded in terms of χ as^[11]

$$\begin{cases} R_T = R_{Tc} + \chi^2 R_{T2} + \dots, & \psi = \sum_{n=1}^{\infty} \psi_n \chi^n, \\ T = \sum_{n=1}^{\infty} T_n \chi^n, & S_1 = \sum_{n=1}^{\infty} S_{1n} \chi^n, & S_2 = \sum_{n=1}^{\infty} S_{2n} \chi^n. \end{cases} \tag{34}$$

The fast time scale t and the slow time scale s are introduced in the form of $s = \chi^2 t$, and hence the operator $\frac{\partial}{\partial t}$ is replaced by the operator $\frac{\partial}{\partial t} + \chi^2 \frac{\partial}{\partial s}$. Substituting Eq. (34) into Eq. (17), we get a set of equations at each order of χ . At the leading order in χ , the coupled differential equation is linear and homogeneous,

$$L \begin{bmatrix} \psi_1 \\ T_1 \\ S_{11} \\ S_{21} \end{bmatrix} = \begin{bmatrix} 0 \\ 0 \\ 0 \\ 0 \end{bmatrix}, \tag{35}$$

which corresponds to the linear instability problem for the oscillatory convection discussed in the previous section. The eigenvalue is $R_T = R_{Tc}^0$, and the eigenfunctions are of the form

$$\psi_1 = (A_1 e^{i\omega t} + \bar{A}_1 e^{-i\omega t}) \sin(\alpha x) \sin(\pi z), \tag{36}$$

$$T_1 = (B_1 e^{i\omega t} + \bar{B}_1 e^{-i\omega t}) \cos(\alpha x) \sin(\pi z), \tag{37}$$

$$S_{11} = (C_1 e^{i\omega t} + \bar{C}_1 e^{-i\omega t}) \cos(\alpha x) \sin(\pi z), \tag{38}$$

$$S_{21} = (D_1 e^{i\omega t} + \bar{D}_1 e^{-i\omega t}) \cos(\alpha x) \sin(\pi z), \tag{39}$$

where the overbar denotes the complex conjugate. The amplitudes $A_1 - D_1$ and $\bar{A}_1 - \bar{D}_1$ are functions of the slow time s , whereas ω and α are taken to be the critical values associated with

$R_T = R_{Tc}^0$. The undetermined amplitudes are related by

$$A_1 = -\frac{\delta^2 + i\omega A}{\alpha} B_1, \quad C_1 = \frac{\delta^2 + i\omega A}{\delta^2 \tau_1 + i\omega} B_1, \quad D_1 = \frac{\delta^2 + i\omega A}{\delta^2 \tau_2 + i\omega} B_1. \tag{40}$$

The inhomogeneous terms appearing in the equations at the order χ^2 are evaluated using the first order solutions,

$$J(\psi_1, T_1) = \frac{\pi\alpha}{2} (B_1 \bar{A}_1 + \bar{B}_1 A_1 + A_1 B_1 e^{2i\omega t} + \bar{A}_1 \bar{B}_1 e^{-2i\omega t}) \sin(2\pi z), \tag{41}$$

$$J(\psi_1, S_{11}) = \frac{\pi\alpha}{2} (C_1 \bar{A}_1 + \bar{C}_1 A_1 + A_1 C_1 e^{2i\omega t} + \bar{A}_1 \bar{C}_1 e^{-2i\omega t}) \sin(2\pi z), \tag{42}$$

$$J(\psi_1, S_{21}) = \frac{\pi\alpha}{2} (D_1 \bar{A}_1 + \bar{D}_1 A_1 + A_1 D_1 e^{2i\omega t} + \bar{A}_1 \bar{D}_1 e^{-2i\omega t}) \sin(2\pi z). \tag{43}$$

From the above relations, we can deduce that the corrections to the stream function, temperature, and solute concentrations fields have terms of the frequency 2ω . Thus, the second order stream function, temperature, and solute concentrations fields can be expressed as follows:

$$\psi_2 = (\psi_{20} + \psi_{22} e^{2i\omega t} + \bar{\psi}_{22} e^{-2i\omega t}) \sin(2\pi z), \tag{44}$$

$$T_2 = (T_{20} + T_{22} e^{2i\omega t} + \bar{T}_{22} e^{-2i\omega t}) \sin(2\pi z), \tag{45}$$

$$S_{12} = (S_{120} + S_{122} e^{2i\omega t} + \bar{S}_{122} e^{-2i\omega t}) \sin(2\pi z), \tag{46}$$

$$S_{22} = (S_{220} + S_{222} e^{2i\omega t} + \bar{S}_{222} e^{-2i\omega t}) \sin(2\pi z), \tag{47}$$

where $(\psi_{20}, \psi_{22}), (T_{20}, T_{22}),$ and $(S_{120}, S_{122}, S_{220}, S_{222})$ are, respectively, the stream functions, the temperatures, and solute concentrations fields which have terms of the frequency 2ω and independent of the fast time scale t .

At the second order in χ , the equation is

$$L \begin{bmatrix} \psi_2 \\ T_2 \\ S_{12} \\ S_{22} \end{bmatrix} = \begin{bmatrix} 0 \\ J(\psi_1, T_1) \\ J(\psi_1, S_{11}) \\ J(\psi_1, S_{21}) \end{bmatrix}. \tag{48}$$

The above equation is now solved, and the solutions are found to be

$$\begin{cases} T_{20} = \frac{\alpha}{8\pi} (A_1 \bar{B}_1 + \bar{A}_1 B_1), & S_{120} = \frac{\alpha}{8\pi \tau_1} (A_1 \bar{C}_1 + \bar{A}_1 C_1), \\ S_{220} = \frac{\alpha}{8\pi \tau_2} (A_1 \bar{D}_1 + \bar{A}_1 D_1), \\ \psi_{20} = 0, & T_{22} = \frac{\pi\alpha A_1 B_1}{8\pi^2 + 4i\omega A}, \\ S_{122} = \frac{\pi\alpha A_1 C_1}{8\pi^2 \tau_1 + 4i\omega}, & S_{222} = \frac{\pi\alpha A_1 D_1}{8\pi^2 \tau_2 + 4i\omega}, \quad \psi_{22} = 0. \end{cases} \tag{49}$$

At the third order in χ , the equation now becomes

$$L \begin{bmatrix} \psi_3 \\ T_3 \\ S_{13} \\ S_{23} \end{bmatrix} = \begin{bmatrix} \Omega \\ A \frac{\partial T_1}{\partial s} + J(\psi_1, T_2) \\ \frac{\partial S_{11}}{\partial s} + J(\psi_1, S_{12}) \\ \frac{\partial S_{21}}{\partial s} + J(\psi_1, S_{22}) \end{bmatrix}, \tag{50}$$

where

$$\Omega = -\frac{\Lambda_1}{Pr_D} \frac{\partial^2}{\partial s \partial t} (\nabla^2 \psi_1) - \Lambda_1 \frac{\partial^2}{\partial s \partial x} (R_{Tc}^0 T_1 - R_{S1} S_{11} - R_{S2} S_{21}) - \Lambda_2 \frac{\partial}{\partial s} (\nabla^2 \psi_1) - \left(1 + \Lambda_1 \frac{\partial}{\partial t}\right) \left(\frac{1}{Pr_D} \frac{\partial}{\partial s} (\nabla^2 \psi_1) + R_{T2} \frac{\partial T_1}{\partial x}\right).$$

The inhomogeneous terms appearing in Eq. (50) are evaluated using the first and second order solutions, and the explicit expressions are given in Appendix A. The third order equations have the solutions

$$\psi_3 = A_3 e^{i\omega t} \sin(\alpha x) \sin(\pi z) + \dots, \tag{51}$$

$$T_3 = B_3 e^{i\omega t} \cos(\alpha x) \sin(\pi z) + \dots, \tag{52}$$

$$S_{13} = C_3 e^{i\omega t} \cos(\alpha x) \sin(\pi z) + \dots, \tag{53}$$

$$S_{23} = D_3 e^{i\omega t} \cos(\alpha x) \sin(\pi z) + \dots. \tag{54}$$

Applying the solvability condition to Eq. (50) yields the following cubic Landau equation:

$$\gamma \frac{dB_1}{ds} = \frac{\alpha^2}{\delta^2} (1 + i\omega \Lambda_1) \Delta_1 R_{T2} B_1 - \eta |B_1|^2 B_1, \tag{55}$$

where

$$\begin{aligned} \gamma = & A + \Lambda_2 \Delta_1 (\delta^2 + i\omega A) - \frac{\alpha^2 \Lambda_1 \Delta_1}{\delta^2} R_{Tc}^0 + \frac{\Delta_1 (1 + 2i\omega \Lambda_1) (\delta^2 + i\omega A)}{Pr_D} \\ & - \left(\frac{\alpha^2 \Delta_1 (1 + i\omega \Lambda_1)}{\delta^2 (\tau_1 \delta^2 + i\omega)} R_{S1} + \frac{\alpha^2 \Delta_1 (1 + i\omega \Lambda_1)}{\delta^2 (\tau_2 \delta^2 + i\omega)} R_{S2} - \frac{\alpha^2 \Delta_1 \Lambda_1}{\delta^2 (\tau_1 \delta^2 + i\omega)} R_{S1} \right) (\delta^2 + i\omega A) \\ & + \frac{\alpha^2 \Delta_1 \Lambda_1 (\delta^2 + i\omega A)}{\delta^2 (\tau_2 \delta^2 + i\omega)} R_{S2} + \frac{\alpha^2 A \Delta_1 (1 + i\omega \Lambda_1)}{\delta^2 (\tau_1 \delta^2 + i\omega)} R_{S1} + \frac{\alpha^2 A \Delta_1 (1 + i\omega \Lambda_1)}{\delta^2 (\tau_2 \delta^2 + i\omega)} R_{S2}, \end{aligned} \tag{56}$$

$$\begin{aligned} \eta = & \frac{\alpha^2 \Delta_1 (1 + i\omega \Lambda_1) (\delta^2 + i\omega A)}{\delta^2 (\tau_1 \delta^2 + i\omega)} \left(\Delta_2 - \frac{(\delta^4 + \omega^2 A^2) (3\pi^2 \delta^2 \tau_1 + i\omega (\delta^2 - \pi^2))}{4(\tau_1^2 \delta^4 + \omega^2) (2\pi^2 \tau_1 + i\omega)} \right) R_{S1} \\ & + \frac{\alpha^2 \Delta_1 (1 + i\omega \Lambda_1) (\delta^2 + i\omega A)}{\delta^2 (\tau_2 \delta^2 + i\omega)} \left(\Delta_2 - \frac{(\delta^4 + \omega^2 A^2) (3\pi^2 \delta^2 \tau_2 + i\omega (\delta^2 - \pi^2))}{4(\tau_2^2 \delta^4 + \omega^2) (2\pi^2 \tau_2 + i\omega)} \right) R_{S2} \\ & + (\delta^2 + i\omega A) \Delta_2 \end{aligned} \tag{57}$$

with

$$\Delta_1 = \frac{Pr_D}{Pr_D (1 + i\omega \Lambda_2) + i\omega (1 + i\omega \Lambda_1)}, \quad \Delta_2 = \frac{3\pi^2 \delta^2 + i\omega A (\delta^2 + \pi^2)}{8\pi^2 + 4i\omega A}.$$

Writing B_1 in the phase-amplitude form,

$$B_1 = |B_1| e^{i\theta}, \tag{58}$$

and substituting this into Eq. (55), we get the following expressions for the amplitude $|B_1|$:

$$\frac{d|B_1|^2}{ds} = 2R_{T2} p_r |B_1|^2 - 2l_r |B_1|^4, \tag{59}$$

$$\frac{d(p_h(B_1))}{ds} = R_{T2} p_i - l_i |B_1|^2, \tag{60}$$

where $(\frac{\alpha^2}{\delta^2}(1 + i\omega\Lambda_1))\Delta_1\gamma^{-1} = p_r + ip_i, \gamma^{-1}\eta = l_r + il_i$, and $p_h(\cdot)$ represents the phase shift. The magnitude and direction of the periodic convective solution and the frequency shift are obtained in Eq. (55). Our curiosity is in the direction of the bifurcation, which is easily shown to be dependent on the sign of the quantity,

$$Q = \frac{l_r}{p_r}. \quad (61)$$

If Q is positive, the bifurcation is supercritical and stable, and it is subcritical and unstable if Q is negative. For this case, the time and area-averaged thermal Nusselt number (Nu_T) and Solute Nusselt numbers (Nu_{S1}, Nu_{S2}) are determined, and they are given by

$$Nu_T = 1 + \frac{\delta^2 p_r}{2 l_r} (R_T - R_{Tc}^0), \quad (62)$$

$$Nu_{Si} = 1 + \frac{\delta^2(\delta^4 + \omega^2 A^2)}{2(\delta^4 \tau_i^2 + \omega^2)} \frac{p_r}{l_r} (R_T - R_{Tc}^0), \quad i = 1, 2. \quad (63)$$

5 Results and discussion

Both linear instability and weakly nonlinear stability of an initially quiescent triply diffusive Oldroyd-B viscoelastic fluid-saturated porous layer are investigated. There are seven nondimensional parameters $Pr_D, \Lambda_1, \Lambda_2, \tau_1, \tau_2, R_{S1}$, and R_{S2} , which influence the stability characteristics of the system, and the thermal Darcy-Rayleigh number is taken as a free parameter. The results are presented for a wide range of the known physical parameters. The value of Pr_D is allowed to vary from 10 to 200 (see Ref. [39]). The viscoelastic parameters Λ_1 and Λ_2 are chosen to be either greater or less than unity^[40]. In particular, the results are also presented for the case of low-density lipoproteins, high-density lipoproteins and triglycerides system for which the diffusion coefficients are, respectively^[41], $\kappa_T = 0.35 \times 10^{-3} \text{ cm}^2/\text{s}$, $\kappa_{S1} = 0.46 \times 10^{-4} \text{ cm}^2/\text{s}$, and $\kappa_{S2} = 0.53 \times 10^{-4} \text{ cm}^2/\text{s}$. The presence of a third diffusing component supports some unusual dynamical behaviours which are not observed in the study of single/double diffusive viscoelastic fluid systems. Some novel results have been delineated by comparing the linear instability characteristics of Oldroyd-B, Maxwell, and Newtonian fluids as particular cases.

5.1 Neutral stability curves

The neutral stability curves in (α, R_T^0) and (α, ω^2) planes for different values of the strain retardation parameter Λ_2 , the Darcy-Prandtl number Pr_D , and the stress relaxation parameter Λ_1 are displayed in Figs. 2–5. It is observed that there exists only one positive value of ω^2 for the parametric values chosen in these figures. The oscillatory neutral stability curves in the (α, R_T^0) plane show an upward concave shape, and the region below each such curve confines to the region of stability, while the region above it corresponds to instability. It is seen that the oscillatory convection occurs even if the ratio of diffusivities is greater than unity, and a reverse result is noticed compared with double diffusive fluid systems (see Fig. 3(a)). Besides, increasing Λ_2 is to increase the value of R_T^0 , indicating that its effect is to enhance the region of stability and also to suppress the frequency of oscillations (see Figs. 2(b) and 3(b)). Moreover, increasing Pr_D (see Fig. 4(a)) and Λ_1 (see Fig. 5(a)) is to decrease the region of stability with the tendency of increasing the frequency of oscillations (see Figs. 4(b) and 5(b)). The results shown in Figs. 6(a) and 6(b) for the case of low-density lipoproteins, high-density lipoproteins and triglycerides system exhibit a similar kind of behaviour as seen in Figs. 2(a) and 2(b). The stabilizing/destabilizing influence of an additional diffusing component on neutral stability curves is displayed in Fig. 7(a) by taking positive/negative values of R_{S1} , respectively, for $Pr_D = 50, A = 2, \Lambda_1 = 0.3, \Lambda_2 = 0.2, \tau_1 = 0.3, \tau_2 = 0.4$, and $R_{S2} = 100$. It is observed that the region of stability increases when the diffusing component is more stabilizing, and also its effect is to suppress the frequency of oscillations (see Fig. 7(b)).

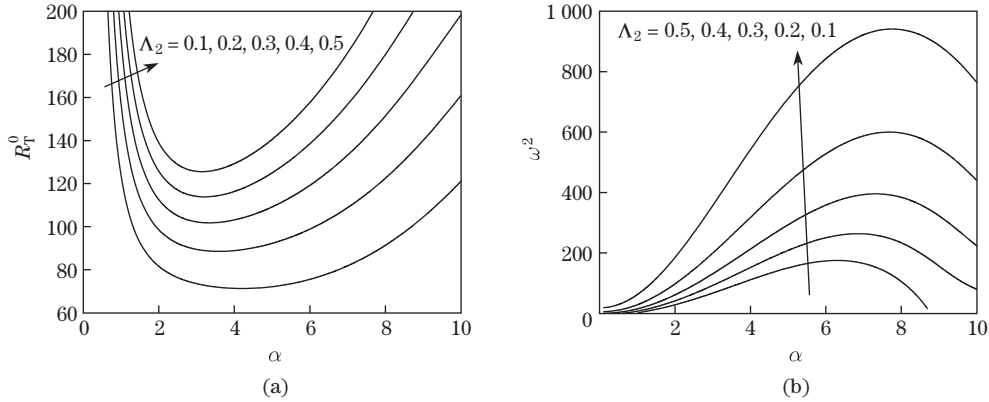


Fig. 2 Neutral stability curves of (a) (α, R_T^0) and (b) (α, ω^2) planes for different values of Λ_2 when $Pr_D = 100, A = 1.78, \tau_1 = 0.208, \tau_2 = 0.244, \Lambda_1 = 0.5, R_{S1} = -20,$ and $R_{S2} = 58$

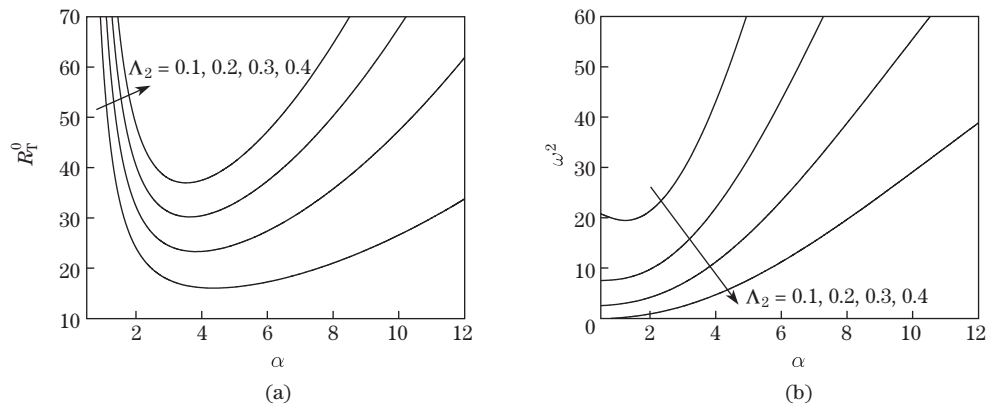


Fig. 3 Neutral stability curves of (a) (α, R_T^0) and (b) (α, ω^2) planes for different values of Λ_2 when $Pr_D = 250, A = 2, \tau_1 = 1.2, \tau_2 = 1.5, \Lambda_1 = 0.6, R_{S1} = -40,$ and $R_{S2} = 55$

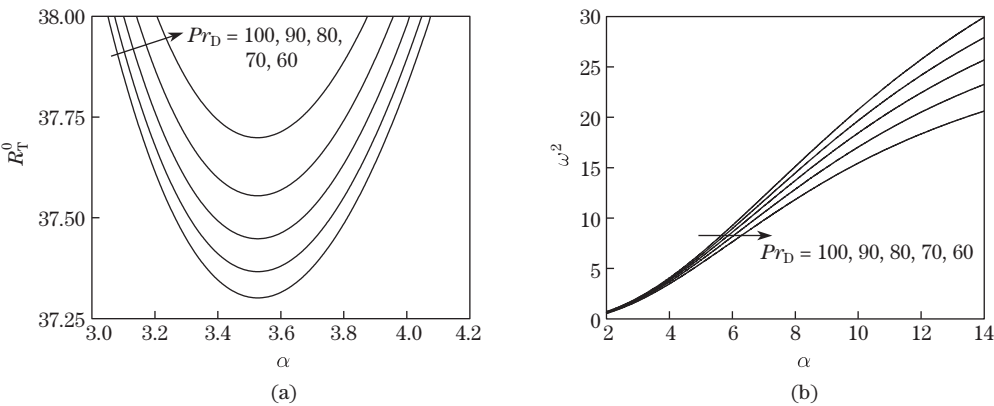


Fig. 4 Neutral stability curves of (a) (α, R_T^0) and (b) (α, ω^2) planes for different values of Pr_D when $A = 2, \Lambda_1 = 0.6, \Lambda_2 = 0.4, \tau_1 = 1.2, \tau_2 = 1.5, R_{S1} = -40,$ and $R_{S2} = 55$

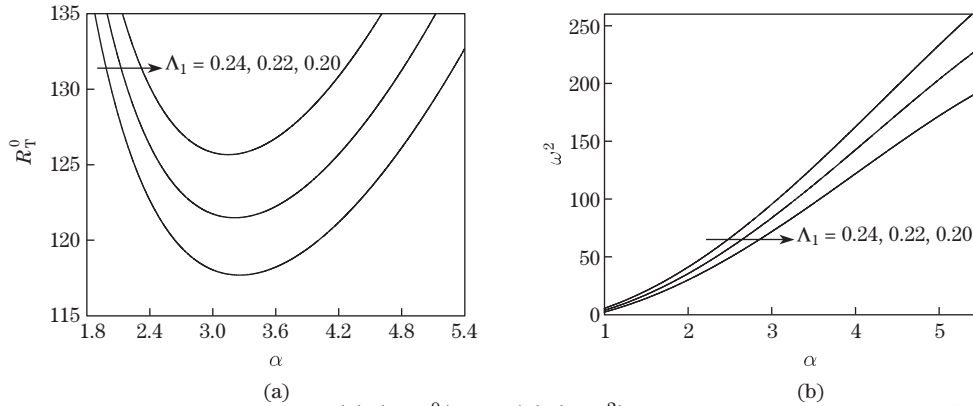


Fig. 5 Neutral stability curves of (a) (α, R_T^0) and (b) (α, ω^2) planes for different values of Λ_1 when $Pr_D = 200$, $A = 1.78$, $\tau_1 = 0.208$, $\tau_2 = 0.244$, $\Lambda_2 = 0.2$, $R_{S1} = -20$, and $R_{S2} = 58$

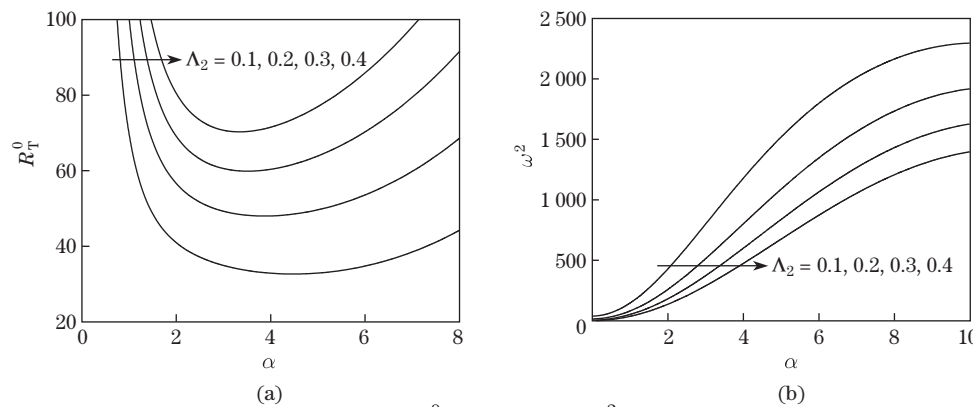


Fig. 6 Neutral stability curves of (a) (α, R_T^0) and (b) (α, ω^2) planes for different values of Λ_2 when $Pr_D = 100$, $A = 1$, $\tau_1 = 0.13$, $\tau_2 = 0.15$, $\Lambda_1 = 0.5$, $R_{S1} = -20$, and $R_{S2} = 58$

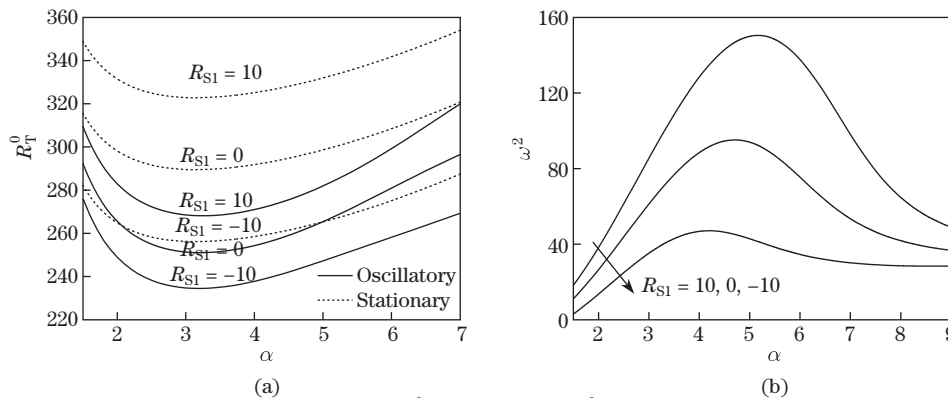


Fig. 7 Neutral stability curves of (a) (α, R_T^0) and (b) (α, ω^2) planes for different values of R_{S1} when $Pr_D = 50$, $A = 2$, $\Lambda_1 = 0.3$, $\Lambda_2 = 0.2$, $\tau_1 = 0.3$, $\tau_2 = 0.4$, and $R_{S2} = 100$

5.2 Disconnected oscillatory neutral curves

The existence of disconnected oscillatory neutral curves under certain conditions is an integral feature of triple diffusive fluid systems which has an important consequence on the linear instability of the system. Such a situation can be obtained by locating the bifurcation points. For this, Eq. (33) has to be solved for any chosen parametric values, which shows that there is a possibility of getting either zero or one/two/three bifurcation points.

The viscoelastic parameters Λ_1 and Λ_2 can be greater than unity for many polymeric fluids, and it is interesting to discern the evolution of neutral stability curves for this case as well. Figures 8(a)–8(f) exhibit evolutions of neutral stability curves for various positive values of R_{S2} ranging from 66.71 to 68 for $Pr_D = 50, A = 1.7, \Lambda_1 = 1.32, \Lambda_2 = 1.2 (\Lambda_1, \Lambda_2 > 1), \tau_1 = 0.191, \tau_2 = 0.264,$ and $R_{S1} = -30$. Figure 8(a) shows that the oscillatory neutral curve is joined to the stationary neutral curve at two bifurcation points. As the value of R_{S2} goes on decreasing, the bifurcation points move closer together and eventually detach from the stationary neutral

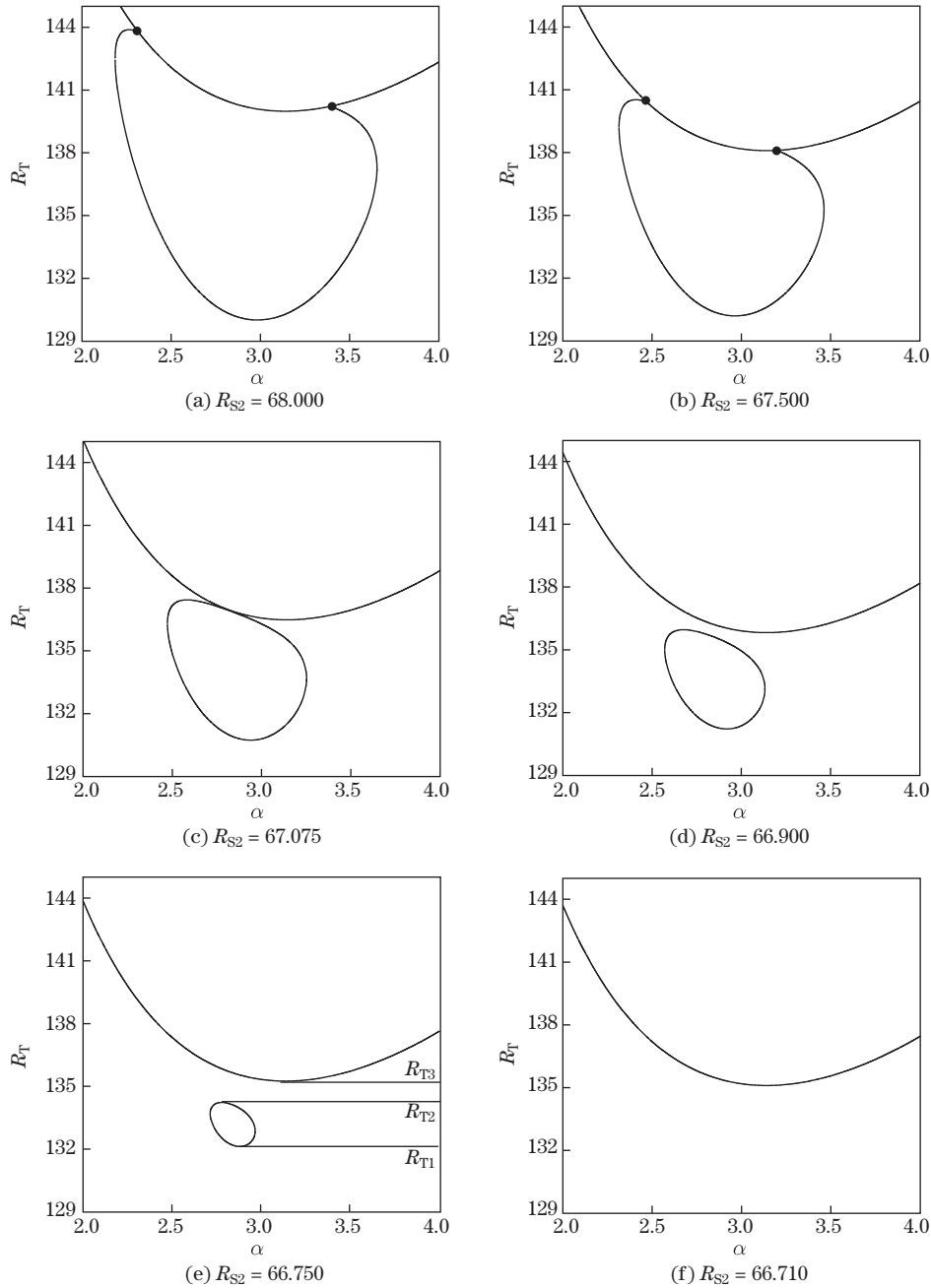


Fig. 8 Evolutions of neutral stability curves with $Pr_D = 50, A = 1.7, \Lambda_1 = 1.32, \Lambda_2 = 1.2, \tau_1 = 0.191, \tau_2 = 0.264,$ and $R_{S1} = -30$

curve (see Figs. 8(b) and 8(c)). Figures 8(b) and 8(c) also show that the left side upper maximum of the closed oscillatory neutral curve lies above the minimum of the steady neutral curve, suggesting that the instability of the system can be conveniently analyzed by a single critical value of R_T . Figure 8(d) shows the complete detachment of the closed convex oscillatory neutral curve from the stationary curve with further decrease in the value of R_{S2} , and when $R_{S2} = 66.75$, the oscillatory curve lies well below the minimum of the stationary neutral curve as shown in Fig. 8(e). Figure 8(e) clearly demonstrates that three critical values of R_T are needed to identify the instability criteria instead of the usual single value. It is seen that the layer is linearly stable if $R_T < R_{T1}$ and $R_{T2} < R_T < R_{T3}$, while for $R_{T1} < R_T < R_{T2}$ and $R_T > R_{T3}$, the layer is unstable. The closed oscillatory neutral curve finally collapses to a point and disappears leaving only the stationary neutral curve when $R_{S2} = 66.71$. It is important to note here that the closed disconnected oscillatory neutral curve is not perfectly heart-shaped, a result that is in contradiction to the Newtonian fluid case^[31] in which the disconnected oscillatory neutral curve has two extrema at the same thermal Darcy-Rayleigh number (i.e., quasiperiodic bifurcation). Thus, we note that this degeneracy is broken due to the presence of viscoelastic effects which contribute in an opposite way on the onset of oscillatory convection.

The critical thermal Darcy-Rayleigh numbers depicting the multivalued region are exhibited in Fig. 9 for the case considered in Fig. 8. To the right of the point A of the infinite slope ($R_{S2} > 67.075$), oscillatory instability first occurs at a lower value of R_{Tc} than the stationary instability, and there is a single value of R_{Tc} . To the left of the point B ($R_{S2} < 66.7242$), instability occurs as the stationary convection, and oscillatory instability does not occur, and again there is one value of R_{Tc} . However, for the finite range of values of R_{S2} lying between the vertical lines passing through the points A and B , three critical values of the thermal Darcy-Rayleigh number are needed to delineate the linear instability criteria.

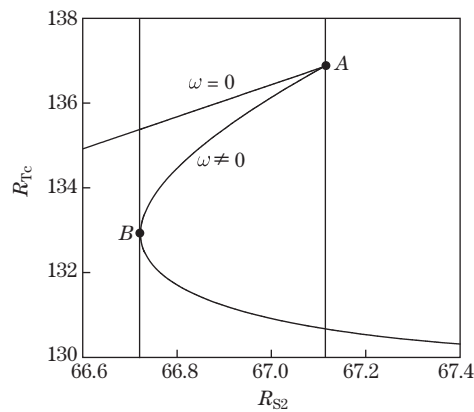


Fig. 9 Stabilities boundary for $Pr_D = 50$, $A = 1.7$, $\Lambda_1 = 1.32$, $\Lambda_2 = 1.2$, $\tau_1 = 0.191$, $\tau_2 = 0.264$, and $R_{S1} = -30$

Figures 10(a)–10(f) represent evolutions of neutral curves for different values of R_{S2} when $Pr_D = 30$, $A = 1.85$, $\Lambda_1 = 0.273$, $\Lambda_2 = 0.173$ ($\Lambda_1, \Lambda_2 < 1$), $\tau_1 = 0.19$, $\tau_2 = 0.273$, and $R_{S1} = -22.50$. The behaviour of neutral curves is similar to that observed in the previous case, but the range of R_{S2} differs in which the disconnected oscillatory neutral curves occur. In this case, the closed convex oscillatory neutral curve goes on dwindling and eventually disappears leaving only the stationary neutral curve at $R_{S2} = 55.3$ (see Fig. 10(f)). Moreover, in this case, the disconnected oscillatory neutral curve is found to be not heart-shaped. The stability boundaries correspond to this case, as shown in Fig. 11.

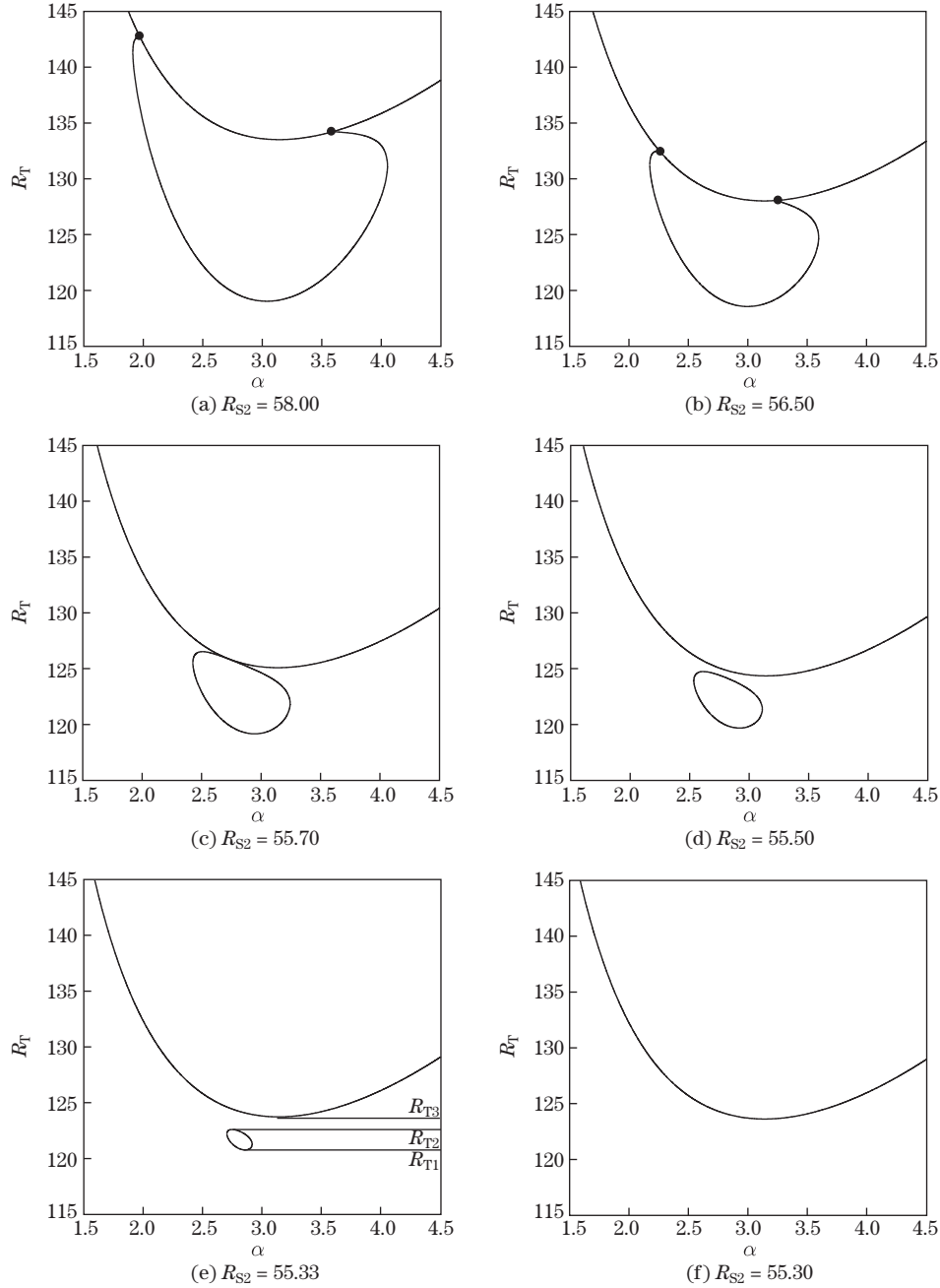


Fig. 10 Evolutions of neutral stability curves with $Pr_D = 30$, $A = 1.85$, $\Lambda_1 = 0.273$, $\Lambda_2 = 0.173$, $\tau_1 = 0.19$, $\tau_2 = 0.273$, and $R_{S1} = -22.50$

It is intriguing to note that the above observed phenomena also carry over to the case of low-density lipoproteins, high-density lipoproteins and triglycerides system as well, and the same phenomenon is evident from Figs. 12(a)–12(f). The results presented here are for $Pr_D = 10$, $A = 1$, $\Lambda_1 = 0.2$, $\Lambda_2 = 0.1$ ($\Lambda_1, \Lambda_2 < 1$), $\tau_1 = 0.13$, $\tau_2 = 0.15$, and $R_{S1} = -10$. These figures indicate that the results are similar to those for the other transport property ratios. From Fig. 12(e), we observe that, the closed convex oscillatory neutral curve has become topologically detached from the stationary neutral curve, demonstrating the requirement of three values of critical thermal

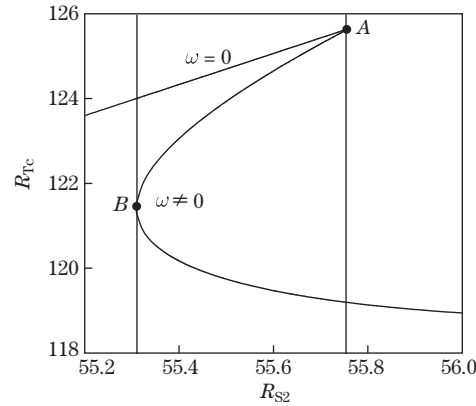


Fig. 11 Stability boundaries for $Pr_D = 30$, $A = 1.85$, $\Lambda_1 = 0.273$, $\Lambda_2 = 0.173$, $\tau_1 = 0.19$, $\tau_2 = 0.273$, and $R_{S1} = -22.50$

Darcy-Rayleigh number to specify the linear instability criteria under certain conditions. Finally, it is seen that the closed convex oscillatory neutral curve collapses to a point and vanishes, leaving only the stationary neutral curve. The corresponding stability boundaries are presented in Fig. 13.

Figures 14 and 15 accomplish the sensitivity of viscoelastic parameters Λ_1 and Λ_2 on the instability characteristics of the system, respectively. Figures 14(a) and 15(a) suggest three values of critical thermal Darcy-Rayleigh number to identify the instability of the system. However, a minor variation in the value of either Λ_1 (see Fig. 14(b)) or Λ_2 (see Fig. 15(b)) completely changes the mode of instability itself. That is to say, the mode of instability switches over from oscillatory to stationary, indicating the adequacy of a single critical thermal Darcy-Rayleigh number to specify the linear instability criteria.

The similarities and differences of the predictions of the two viscoelastic models as well as the Newtonian fluid are enunciated in Figs. 16(a)–16(c). Figures 16(a), 16(b), and 16(c), respectively, display the nature of neutral stability curves for Oldroyd-B ($\Lambda_1 = 0.15$, $\Lambda_2 = 0.1$), Maxwell ($\Lambda_1 = 0.15$, $\Lambda_2 = 0$) and Newtonian ($\Lambda_1 = \Lambda_2 = 0$) fluids with $Pr_D = 30$, $A = 2$, $\tau_1 = 0.201$, $\tau_2 = 0.249$, $R_{S1} = -23$, and $R_{S2} = 48.5$. In the case of an Oldroyd-B fluid, three critical thermal Darcy-Rayleigh numbers are required to specify the linear instability criteria, while in the case of remaining two types of fluids, a single critical thermal Darcy-Rayleigh number is enough to describe the linear instability. Moreover, the onset of instability ceases to be oscillatory in the case of Newtonian fluids, and it is seen that the instability sets in as only stationary convection.

5.3 Critical condition

Analyzing the behaviour of critical thermal Darcy-Rayleigh number R_{Tc} and the corresponding critical frequency of oscillations ω_c for various physical parameters is important as it provides the crucial information on the linear instability of the system. The variations of R_{Tc} and ω_c as a function of Λ_2 are shown in Figs. 17(a) and 17(b), respectively, for different values of Λ_1 when $A = 1.78$, $\tau_1 = 0.208$, $\tau_2 = 0.244$, $R_{S1} = -20$, and $R_{S2} = 30$. Figure 17(a) clearly exposes the dual effect of elasticity parameters on the nature of onset of instability. It is seen that, for a fixed value of Λ_1 , there exists a threshold value of Λ_2 below which the instability first sets in as oscillatory convection and beyond which stationary convection is preferred. Moreover, the threshold value of Λ_2 increases with increasing Λ_1 . The onset of oscillatory convection gets delayed with increasing Λ_2 while the trend gets reversed with increasing Λ_1 . This is because the increase in Λ_2 amounts to the increase in the time taken by the fluid element to respond to the

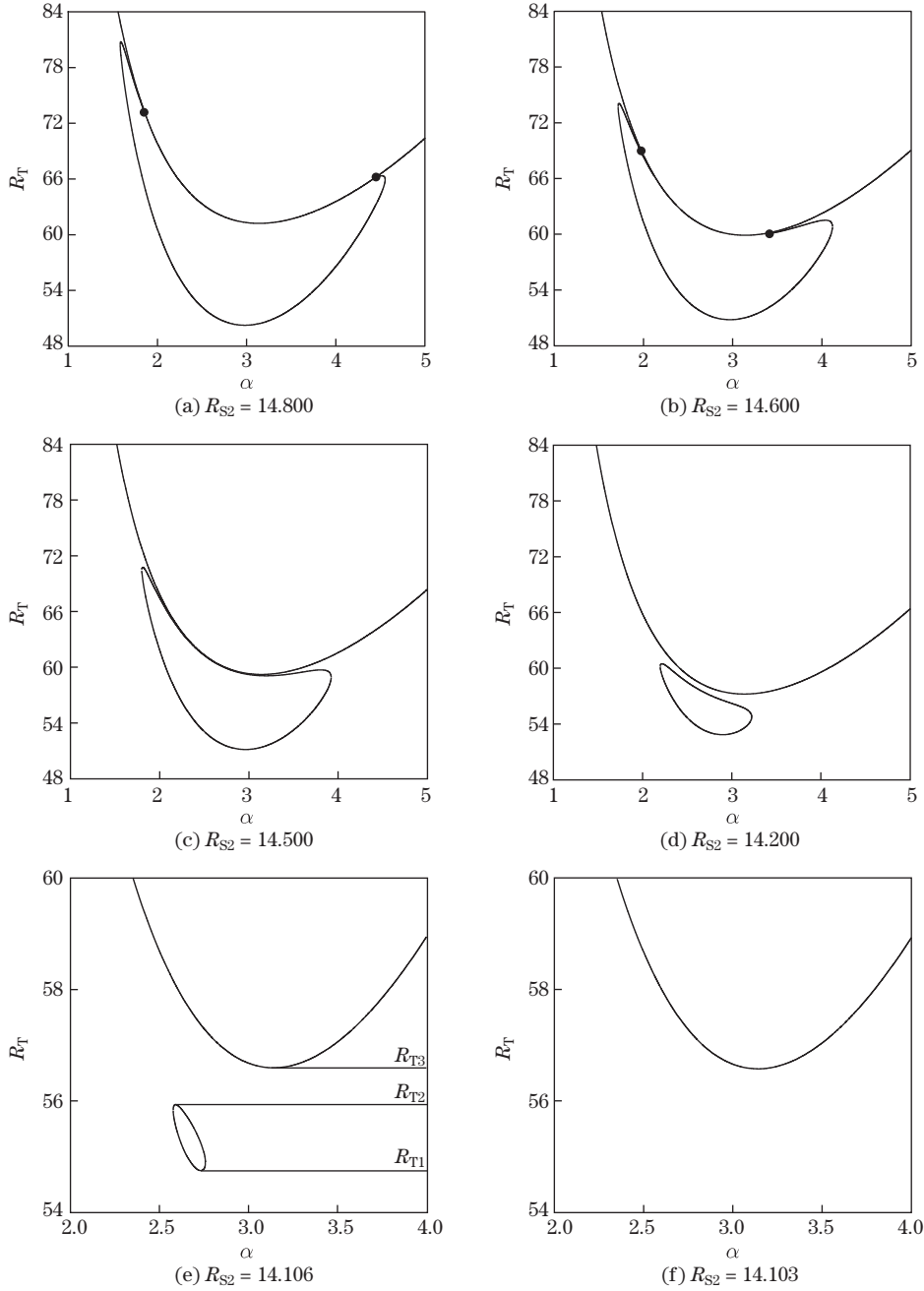


Fig. 12 Evolutions of neutral stability curves with $Pr_D = 10$, $A = 1$, $\Lambda_1 = 0.2$, $\Lambda_2 = 0.1$, $\tau_1 = 0.13$, $\tau_2 = 0.15$, and $R_{S1} = -10$

applied stress. That is, during the growth of the retardation parameter, the effect of friction will be higher, and as a result higher values of R_{TC} are needed to instil instability on the system with increasing Λ_2 . Whereas the increase in Λ_1 amounts to allowing the applied stress to act for a longer time on the fluid element which results in lesser elastic memory of the fluid. In fact, the increase of relaxation ceases the stickiness of the fluid, and hence the effect of friction will be lesser so that the convection sets in at lower values of R_{TC} with increasing Λ_1 . The opposite

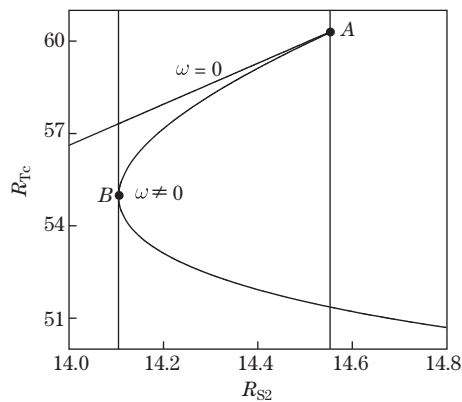


Fig. 13 Stability boundaries for $Pr_D = 10$, $A = 1$, $\Lambda_1 = 0.2$, $\Lambda_2 = 0.1$, $\tau_1 = 0.13$, $\tau_2 = 0.15$, and $R_{S1} = -10$

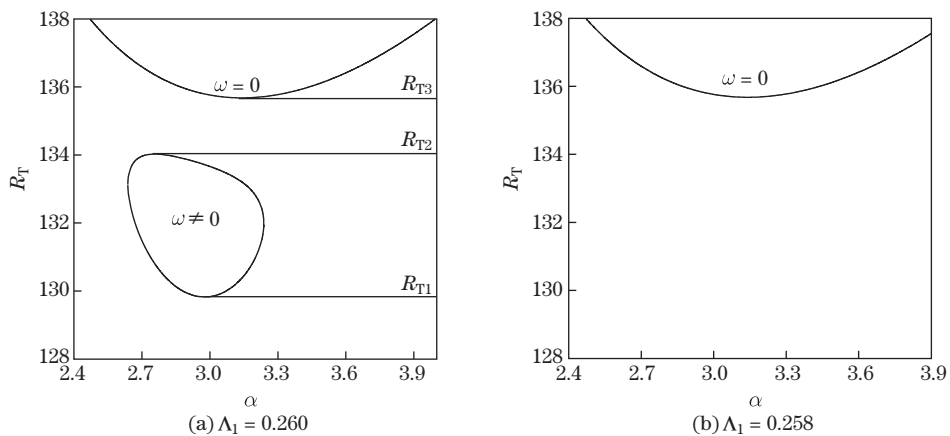


Fig. 14 Variations of the relaxation parameter Λ_1 on evolutions of neutral stability curves for $Pr_D = 25$, $A = 2$, $\Lambda_2 = 0.2$, $\tau_1 = 0.2$, $\tau_2 = 0.2588$, $R_{S1} = -22.8$, and $R_{S2} = 54.4$

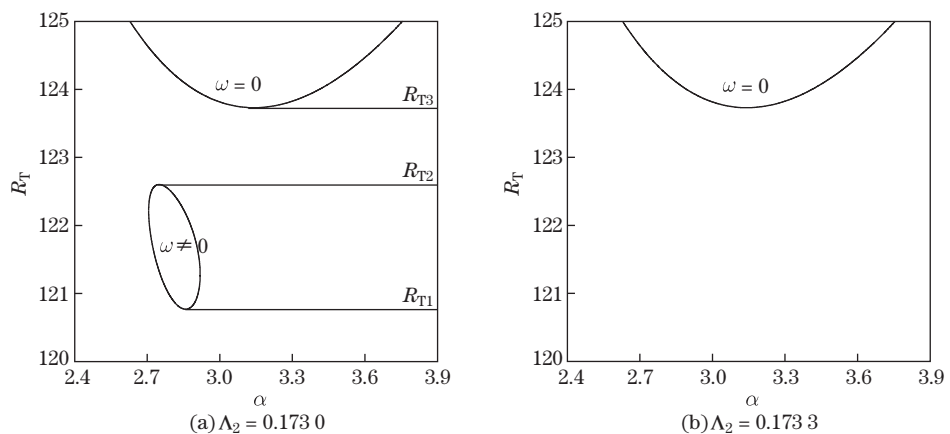


Fig. 15 Variations of the retardation parameter Λ_2 on evolutions of neutral stability curves for $Pr_D = 30$, $A = 1.85$, $\Lambda_1 = 0.273$, $\tau_1 = 0.19$, $\tau_2 = 0.273$, $R_{S1} = -22.50$, and $R_{S2} = 55.33$

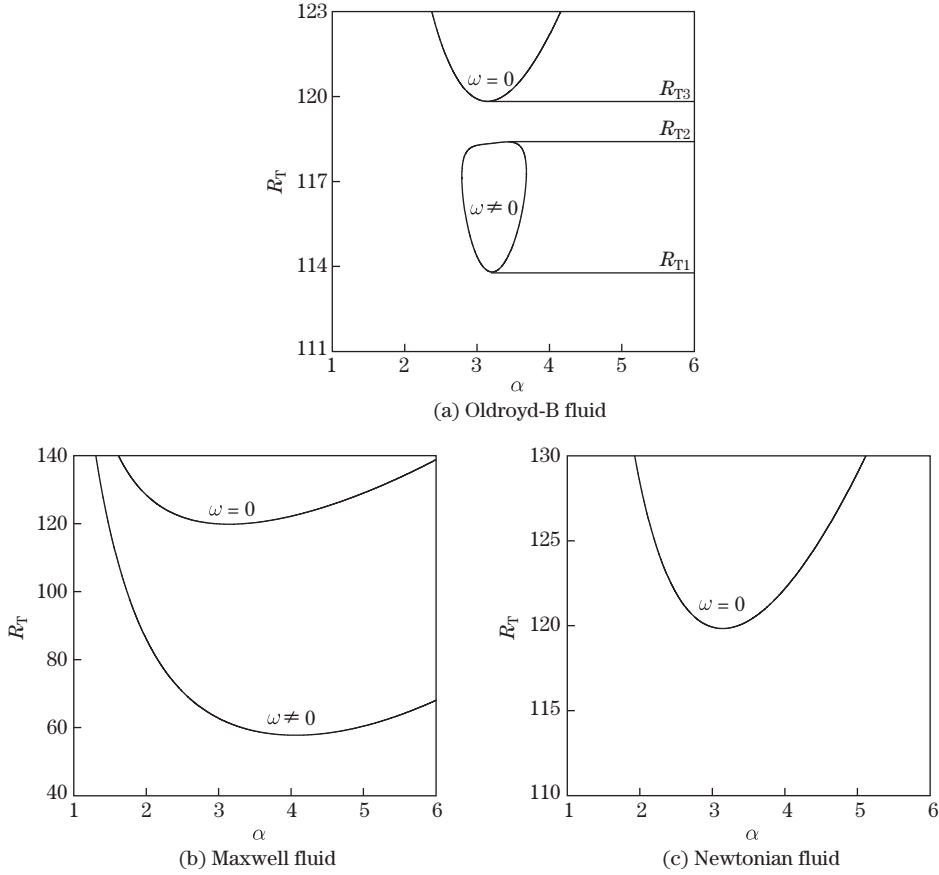


Fig. 16 Instability characteristics in the (α, R_T) plane for (a) Oldroyd-B fluid, $\Lambda_1 = 0.15, \Lambda_2 = 0.1$, (b) Maxwell fluid, $\Lambda_1 = 0.15, \Lambda_2 = 0$, and (c) Newtonian fluid, $\Lambda_1 = \Lambda_2 = 0$, when $Pr_D = 30$, $A = 2$, $\tau_1 = 0.201$, $\tau_2 = 0.249$, $R_{S1} = -23$, and $R_{S2} = 48.5$

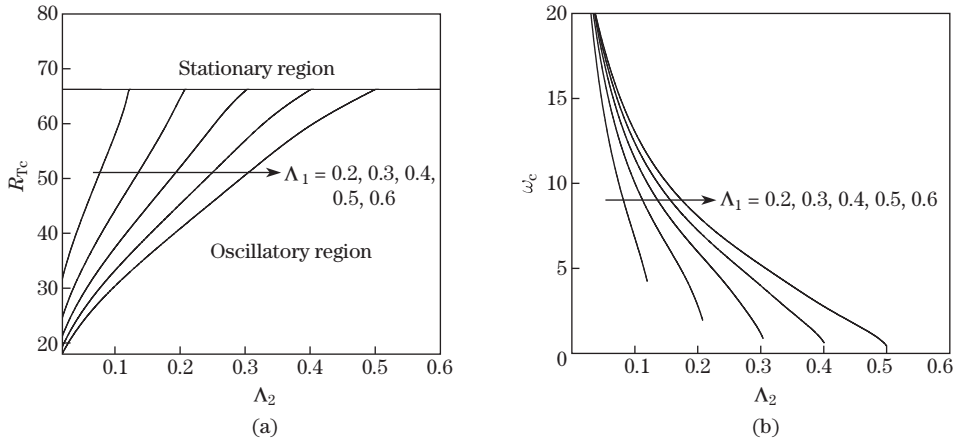


Fig. 17 Variations of (a) R_{Tc} and (b) ω_c with Λ_2 for different values of Λ_1 when $Pr_D = 200$, $A = 1.78$, $\tau_1 = 0.208$, $\tau_2 = 0.244$, $R_{S1} = -20$, and $R_{S2} = 30$

behaviour of elasticity parameters on the onset of oscillatory convection is also seen through the variation in ω_c shown in Fig. 17(b). From this figure, it is observed that ω_c increases with

increasing Λ_1 due to an increase in the elasticity of the fluid, and an opposite behaviour could be seen with increasing Λ_2 . Thus, it is evident that the increase in the overstability vibration is to advance the onset of oscillatory convection. In Fig. 18, we display the effect of Darcy-Prandtl number Pr_D on the critical thermal Darcy-Rayleigh number R_{Tc} . We observe that the effect of increasing Pr_D is to increase the range of threshold value of Λ_2 at which the instability switches over from oscillatory to stationary and also to hasten the onset of oscillatory convection.

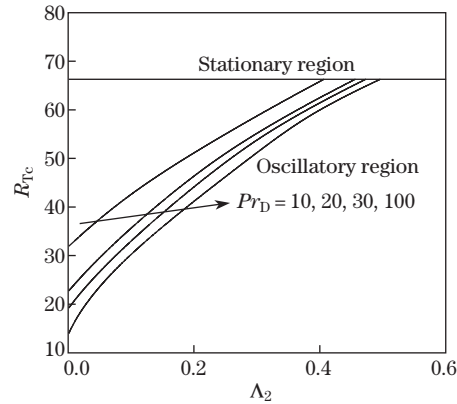


Fig. 18 Variations of R_{Tc} with Λ_2 for different values of Pr_D when $A = 1.78$, $\Lambda_1 = 0.6$, $\tau_1 = 0.208$, $\tau_2 = 0.244$, $R_{S1} = -20$, and $R_{S2} = 30$

It is possible to estimate R_{Tc} for both stationary and oscillatory convections which coincide for some parametric values, and as a result, a codimension-two bifurcation occurs. This behaviour is illustrated in Fig. 19 on the $(\Lambda_2/\Lambda_1, \Lambda_1)$ plane for different known values of Pr_D obtained from Eqs. (26) and (28). In the figure, each curve locates the boundary separating stationary and oscillatory solution regions. For fixed values of Λ_2/Λ_1 and Pr_D , there exists a value of $\Lambda_1 = \Lambda_1^*$, where $R_{Tc}^S = R_{Tc}^O$. The system is unstable under oscillatory convection in the region above each curve, and below the curve, the system is unstable under stationary convection. For a fixed value of Λ_2/Λ_1 , the value of Λ_1 at which a codimension-two bifurcation occurs decreases with increasing Pr_D .

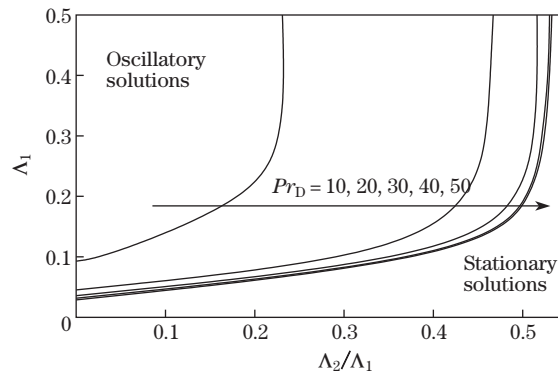


Fig. 19 Bifurcations of stationary and oscillatory solutions in the viscoelastic parameter plane for different values of Pr_D when $A = 1$, $\tau_1 = 0.2$, $\tau_2 = 0.3$, $R_{S1} = -140$, and $R_{S2} = 223$

5.4 Oscillatory nonlinear stability

The stability of oscillatory bifurcating solutions is analyzed by deriving a cubic Landau equation. The nature of oscillatory bifurcation can be determined from the sign of Q , and

the point at which Q changes the sign is termed as the point. Figures 20–22 represent the computed values of Q as a function of R_{S2} for different values of physical parameters, namely, $Pr_D, R_{S1}, \Lambda_1, \Lambda_2, \tau_1,$ and τ_2 . These figures demonstrate the possibility of subcritical oscillatory bifurcation for a range of parametric values, and indicate the occurrence of instability before the linear threshold is reached. This is expected, because the linear instability analysis only provides a sufficient condition for instability. Besides, the tricritical point is shifted towards higher values of R_{S2} with increasing $\Lambda_1, R_{S1},$ and $\tau_2,$ while an opposite trend could be seen with increasing $Pr_D, \Lambda_2,$ and τ_1 .

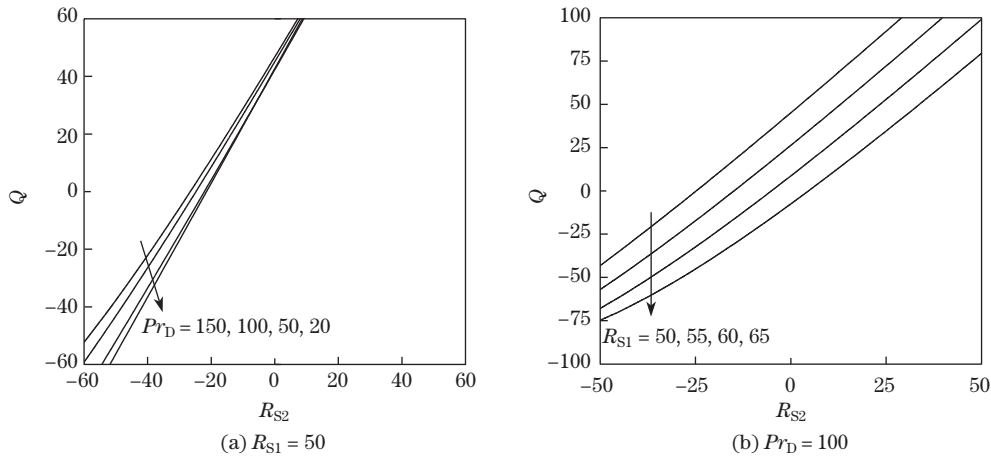


Fig. 20 Variations of Q as a function of R_{S2} for different values of Pr_D and R_{S1} when $A = 1,$ $\Lambda_1 = 1.2, \Lambda_2 = 1, \tau_1 = 0.8,$ and $\tau_2 = 1.2$

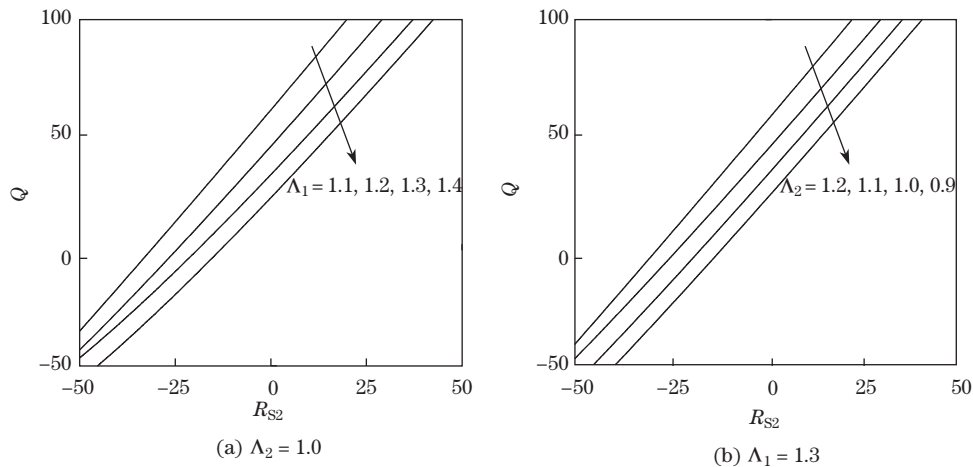


Fig. 21 Variations of Q as a function of R_{S2} for different values of Λ_1 and Λ_2 when $A = 1, Pr_D = 120,$ $\tau_1 = 0.8, \tau_2 = 1.2,$ and $R_{S1} = 50$

5.5 Heat and mass transport

Heat and mass transfer are measured through thermal and solute Nusselt numbers. The thermal Nusselt number (Nu_T) and solute Nusselt numbers (Nu_{S1}, Nu_{S2}) are displayed as a function of R_T for different values of $Pr_D, \Lambda_1,$ and Λ_2 in Figs. 23(a), 23(b), and 23(c),

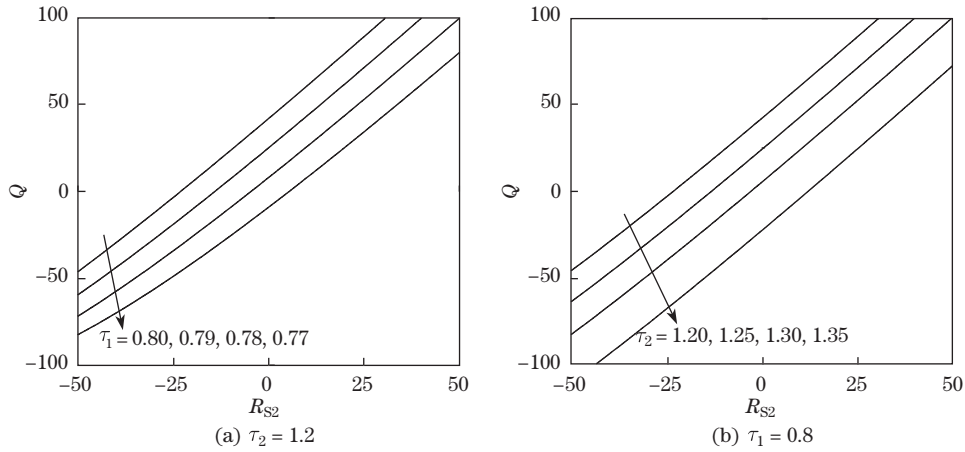


Fig. 22 Variations of Q as a function of R_{S2} for different values of τ_1 and τ_2 when $A = 1$, $Pr_D = 120$, $\Lambda_1 = 1.2$, $\Lambda_2 = 1$, and $R_{S1} = 50$

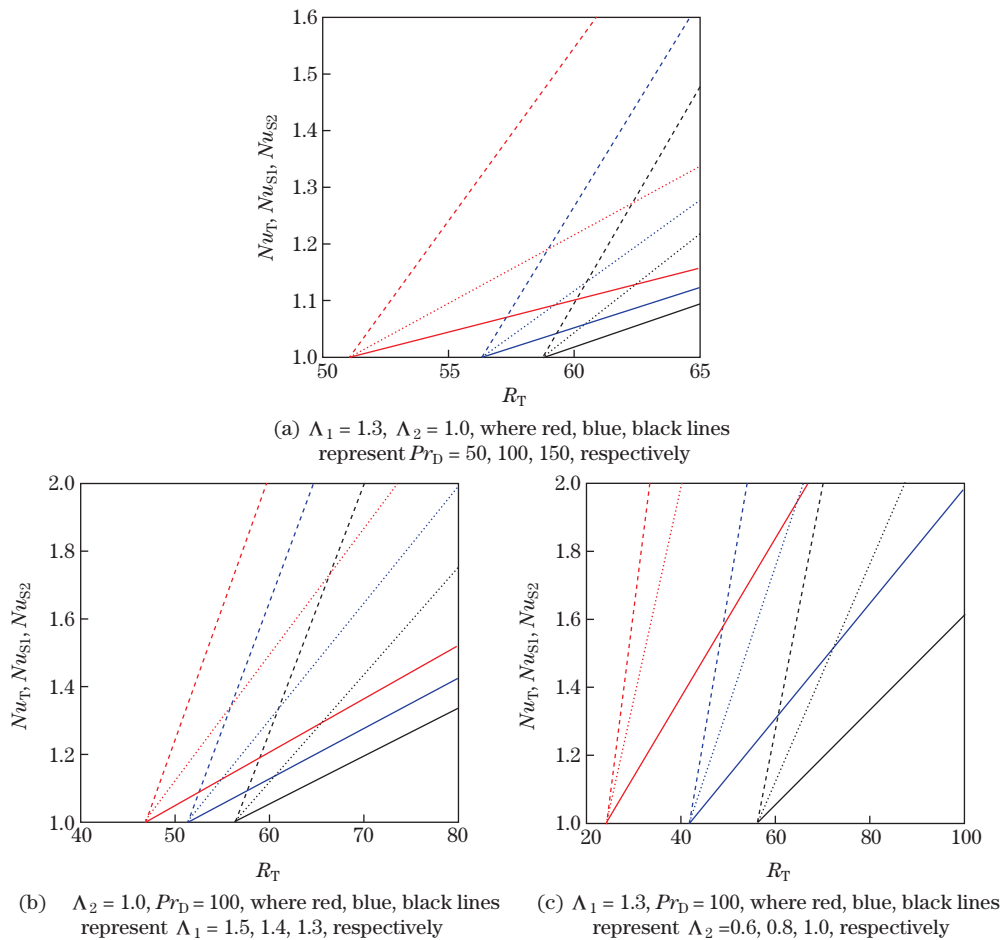


Fig. 23 Time and area-averaged Nusselt numbers Nu_T (solid lines), Nu_{S1} (dashed lines), and Nu_{S2} (dotted lines) for different values of Pr_D , Λ_1 , and Λ_2 when $A = 2$, $\tau_1 = 0.2$, $\tau_2 = 1.0$, $R_{S1} = 50$, and $R_{S2} = -50$ (color online)

respectively. The increase in the value of Λ_1 is to increase the heat and mass transfer characteristics of oscillatory convection, whereas the increase in Λ_2 and Pr_D exhibits an opposite kind of behaviour. This may be attributed to the fact that the increase in Λ_1 is to increase the overstability vibration (see Figs. 5(b) and 17(b)), and consequently, its effect is to enhance the heat and mass transfer, while the increase in Λ_2 is to suppress the heat and mass transfer because their effect is to decrease the overstability vibration (see Figs. 3(b) and 17(b)).

6 Conclusions

The triple diffusive convection in an Oldroyd-B fluid-saturated porous medium is investigated. By performing the linear instability analysis, the condition for the onset of stationary and oscillatory convection is established. It is found that the oscillatory convection occurs even if the ratio of diffusivities is greater than unity. Under certain conditions, disconnected closed convex oscillatory neutral curves are found to occur, indicating the requirement of three critical thermal Darcy-Rayleigh numbers to specify the linear instability criteria instead of the usual single value. This result is in contradiction to the observed phenomenon for Newtonian fluids wherein the disconnected oscillatory neutral curve is found to be perfectly heart-shaped (i.e., quasiperiodic bifurcation). The effect of increasing retardation parameter is to delay the onset of oscillatory convection, while the trend gets reversed with the increasing relaxation parameter. The value of retardation parameter beyond which the instability sets in as oscillatory convection increases with the increasing relaxation parameter as well as the Darcy-Prandtl number. The instability characteristics of the system analyzed under the same parametric values for Oldroyd-B, Maxwell, and Newtonian fluids are found to be qualitatively different. A perturbation method is used to perform a weakly nonlinear stability analysis, and subcritical bifurcation is found to be possible depending on the choice of physical parameters. Also, the increase in the value of the relaxation parameter is to enhance the time and area-averaged heat and mass transfer, while the increase in the retardation parameter and the Darcy-Prandtl number exhibits an opposite kind of performance.

Acknowledgements The authors thank reviewers for their constructive remarks and useful suggestions, which improve the work significantly.

References

- [1] HORTON, C. W. and ROGERS, F. T. Convection currents in a porous medium. *Journal of Applied Physics*, **16**, 367–370 (1945)
- [2] LAPWOOD, E. R. Convection of a fluid in a porous medium. *Mathematical Proceedings of the Cambridge Philosophical Society*, **44**, 508–512 (1948)
- [3] NIELD, D. A. and BEJAN, A. *Convection in Porous Media*, 5th ed., Springer, New York (2017)
- [4] STRAUGHAN, B. *Stability and Wave Motion in Porous Media*, Springer, New York (2008)
- [5] STRAUGHAN, B. *Convection with Local Thermal Non-Equilibrium and Microfluidic Effects*, Springer, New York (2015)
- [6] VAFAI, K. *Handbook of Porous Media*, Marcel Dekker, New York (2000)
- [7] RUDRAIAH, N., SRIMANI, P. K., and FRIEDRICH, R. Finite amplitude convection in a two-component fluid saturated porous layer. *International Journal of Heat and Mass Transfer*, **25**, 715–722 (1982)
- [8] KIM, M. C., LEE, S. B., KIM, S., and CHUNG, B. J. Thermal instability of viscoelastic fluids in porous media. *International Journal of Heat and Mass Transfer*, **46**, 5065–5072 (2003)
- [9] SHIVAKUMARA, I. S. and SURESHKUMAR, S. Convective instabilities in a viscoelastic-fluid-saturated porous medium with through flow. *Journal of Geophysics and Engineering*, **4**, 104–115 (2007)

-
- [10] BERTOLA, V. and CAFARO, E. Thermal instability of viscoelastic fluids in horizontal porous layers as initial problem. *International Journal of Heat and Mass Transfer*, **4**, 4003–4012 (2006)
- [11] WANG, S. and TAN, W. Stability analysis of solet-driven double-diffusive convection of Maxwell fluid in a saturated porous medium. *International Journal of Heat and Fluid Flow*, **32**, 88–94 (2011)
- [12] MALASHETTY, M. S., TAN, W. C., and SWAMY, M. The onset of double diffusive convection in a binary viscoelastic fluid saturated anisotropic porous layer. *Physics of Fluids*, **21**, 084101–084111 (2009)
- [13] AWAD, F. G., SIBANDA, P., and MOTSA, S. S. On the linear stability analysis of a Maxwell fluid with double-diffusive convection. *Applied Mathematical Modeling*, **34**, 3509–3517 (2010)
- [14] LARSON, R. G. Instabilities in viscoelastic flows. *Rheological Acta*, **31**, 213–221 (1992)
- [15] PERKINS, T. T., QUAKE, S. R., SMITH, D. E., and CHU, S. Relaxation of a single DNA molecule observed by optical microscopy. *Science*, **264**, 822–826 (1994)
- [16] PERKINS, T. T., SMITH, D. E., and CHU, S. Single polymer dynamics in an elongational flow. *Science*, **276**, 2016–2021 (1997)
- [17] KOLODNER, P. Oscillatory convection in viscoelastic DNA suspensions. *Journal of Non-Newtonian Fluid Mechanics*, **75**, 167–192 (1998)
- [18] CELIA, M. A., KINDRED, J. S., and HERRERA, I. Contaminant transport and biodegradation I: a numerical model for reactive transport in porous media. *Water Resources Research*, **25**, 1141–1148 (1989)
- [19] CHEN, B., CUNNINGHAM, A., EWING, R., PERALTA, R., and VISSER, E. Two-dimensional modelling of micro scale transport and biotransformation in porous media. *Numerical Methods Partial Differential Equations*, **10**, 65–83 (1994)
- [20] GRIFFITHS, R. W. The transport of multiple components through thermohaline diffusive interfaces. *Deep-Sea Research*, **26**, 383–397 (1979)
- [21] TURNER, J. S. Multicomponent convection. *Annual Review of Fluid Mechanics*, **17**, 11–44 (1985)
- [22] MOROZ, I. M. Multiple instabilities in a triply diffusive system. *Studies in Applied Mathematics*, **80**, 137–164 (1989)
- [23] COX, S. M. and MOROZ, I. M. Multiple bifurcations in triple convection with non-ideal boundary conditions. *Physica D: Nonlinear Phenomena*, **93**, 1–22 (1996)
- [24] PEARLSTEIN, A. J., HARRIS, R. M., and TERRONES, G. The onset of convective instability in a triply diffusive of fluid layer. *Journal of Fluid Mechanics*, **202**, 443–465 (1989)
- [25] TERRONES, G. and PEARLSTEIN, A. J. The onset of convection in a multicomponent fluid layer. *Physics of Fluids*, **1**, 845–853 (1989)
- [26] TERRONES, G. Cross diffusion effects on the stability criteria in a triply diffusive system. *Physics of Fluids*, **5**, 2172–2182 (1993)
- [27] LOPEZ, A. R., ROMERO, L. A., and PEARLSTEIN, A. J. Effect of rigid boundaries on the onset of convective instability in a triply diffusive fluid layer. *Physics of Fluids*, **2**, 896–902 (1990)
- [28] SHIVAKUMARA, I. S. and NAVEEN-KUMAR, S. B. Linear and weakly nonlinear triple diffusive convection in a couple stress fluid layer. *International Journal of Heat and Mass Transfer*, **68**, 542–553 (2015)
- [29] RUDRAIAH, N. and VORTMEYER, D. Influence of permeability and of a third diffusing component upon the onset of convection in a porous medium. *International Journal of Heat and Mass Transfer*, **25**, 457–464 (1982)
- [30] POULIKAKOS, D. Effect of a third diffusing component on the onset of convection in a horizontal layer. *Physics of Fluids*, **28**, 3172–3174 (1985)
- [31] TRACEY, J. Multi-component convection-diffusion in a porous medium. *Continuum Mechanics and Thermodynamics*, **8**, 361–381 (1996)
- [32] RIONERO, S. Long-time behaviour of multi-component fluid mixtures in porous media. *International Journal of Engineering Science*, **48**, 1519–1533 (2010)
- [33] RIONERO, S. Triple diffusive convection in porous media. *Acta Mechanica*, **224**, 447–458 (2003)

- [34] ZHAO, M., WANG, S., and ZHANG, Q. Onset of triply diffusive convection in a Maxwell fluid saturated porous layer. *Applied Mathematical Modeling*, **38**, 2345–2352 (2014)
- [35] RAGHUNATHA, K. R., SHIVAKUMARA, I. S., and SHANKAR, B. M. Weakly nonlinear stability analysis of triple diffusive convection in a Maxwell fluid saturated porous layer. *Applied Mathematics and Mechanics (English Edition)*, **39**, 153–168 (2018) <https://doi.org/10.1007/s10483-018-2298-6>
- [36] ALISHAEV, M. G. and MIRZADJANZADE, A. K. For the calculation of delay phenomenon in filtration theory. *Izvestiya Vuzov Nef't'i Gaz*, **6**, 71–77 (1975)
- [37] KHUZHAVOROV, B., AURIAULT, J. L., and ROVER, P. Derivation of macroscopic filtration law for transient linear viscoelastic fluid flow in porous media. *International Journal of Engineering Science*, **38**, 487–504 (2000)
- [38] TAN, W. and MASUOKA, T. Stability analysis of a Maxwell fluid in a porous medium heated from below. *Physics Letters A*, **360**, 454–460 (2007)
- [39] VADASZ, P. Coriolis effect on gravity-driven convection in a rotating porous layer heated from below. *Journal of Fluid Mechanics*, **376**, 351–375 (1998)
- [40] PLUTCHOK, G. J. and JOZEF, L. K. Predicting steady and oscillatory shear rheological properties of CMC and guar gum blends from concentration and molecular weight data. *Journal of Food Science*, **51**, 1284–1288 (1986)
- [41] HAO, W. and FRIEDMAN, A. The LDL-HDL profile determines the risk of atherosclerosis: a mathematical model. *PLoS One*, **9**, 1–15 (2014)

Appendix A

The inhomogeneous terms appearing in the third order equations are calculated using the first and second order solutions,

$$\begin{aligned} \Omega &= \left(\left(\delta^2 \Lambda_2 + \frac{\delta^2 (1 + 2i\omega \Lambda_1)}{Pr_D} \right) \frac{dA_1}{ds} + \alpha (\Lambda_1 R_{Tc}^0 + (1 + i\omega \Lambda_1) R_{T2}) \frac{dB_1}{ds} \right) e^{i\omega t} \sin(\alpha x) \sin(\pi z) \\ &\quad - \left(\alpha \Lambda_1 R_{S1} \frac{dC_1}{ds} + \alpha \Lambda_1 R_{S2} \frac{dD_1}{ds} \right) e^{i\omega t} \sin(\alpha x) \sin(\pi z) + \dots, \\ A \frac{\partial T_1}{\partial s} + J(\psi_1, T_2) &= -\pi^2 \alpha^2 \left(\frac{(A_1 \bar{B}_1 + \bar{A}_1 B_1) A_1}{8\pi^2} + \frac{B_1 A_1 \bar{A}_1}{(8\pi^2 + 4iA\omega)} \right) e^{i\omega t} \cos(\alpha x) \sin(\pi z) + \dots, \\ \frac{\partial S_{11}}{\partial s} + J(\psi_1, S_{12}) &= -\pi^2 \alpha^2 \left(\frac{(A_1 \bar{C}_1 + \bar{A}_1 C_1) A_1}{8\pi^2 \tau_1} + \frac{C_1 A_1 \bar{A}_1}{(8\pi^2 \tau_1 + 4i\omega)} \right) e^{i\omega t} \cos(\alpha x) \sin(\pi z) + \dots, \\ \frac{\partial S_{21}}{\partial s} + J(\psi_1, S_{22}) &= -\pi^2 \alpha^2 \left(\frac{(A_1 \bar{D}_1 + \bar{A}_1 D_1) A_1}{8\pi^2 \tau_2} + \frac{D_1 A_1 \bar{A}_1}{(8\pi^2 \tau_2 + 4i\omega)} \right) e^{i\omega t} \cos(\alpha x) \sin(\pi z) + \dots. \end{aligned}$$